# Functional expression and initial biochemical characterization of

# Yp-NhaP, cation-proton antiporter from Yersinia pestis

By

Talal Abboud

A thesis submitted to the Faculty of Graduate Studies

of the University Of Manitoba

in partial fulfilment of the requirements for the degree of

**Master of Science**

**Department of Microbiology**

**University of Manitoba**

**Winnipeg, Manitoba**

# Abstract

The major objectives of this work were cloning, functional expression and primary biochemical characterization of Yp-NhaP, putative sodium-proton antiporter from the dangerous human pathogen *Yersinia pestis*.

We expressed Yp-NhaP in its functional form in the antiporter-deficient strain of *E. coli*, TO114. When assayed in inside-out sub-bacterial membrane vesicles, Yp-NhaP acted as an electroneutral cation/proton antiporter, exchanging $Ca^{2+}$, $K^+$, $Na^+$ and $Li^+$ ions for $H^+$.

Competition experiments suggested that *in vivo* Yp-NhaP operates as $Ca^{2+}/H^+$ and, possibly, $Ca^{2+}/Na^+$ antiporter rather than $K^+/H^+$ or $Na^+/H^+$ antiporter. $Ca^{2+}/H^+$ and $Li^+/H^+$ antiport catalyzed by Yp-NhaP peaked at pH close to 8.0, while $K^+/H^+$ and $Na^+/H^+$ antiport were smoothly increasing from pH 6.5 to pH 9.0. We also observed inhibition by the excess of substrate in the case of $Ca^{2+}/H^+$ and $Li^+/H^+$ antiport mediated by Yp-NhaP.

As expected, chromosomal deletion of *Yp-nhaP* gene did not affect resistance of *Y. pestis* cells to alkali cations.

**Acknowledgements**

I would like to thank my supervisor, Dr. Pavel Dibrov for his support and mentorship.

Many thanks are due to Dr. Claudia C. Häse and Mr. Matthew Quinn (Oregon State University) for providing us with the *nhaP* chromosomal deletion mutant of *Y. pestis*. I would also like to thank Dr. Judith Winogrodzki, Mr. Craig Resch and Mr. Curtis Patterson for their help in the lab and support.

My special thanks are to the members of my Advising Committee, Dr. Deborah Court (Dept. of Microbiology) and Dr. Mazdak Khajehpour (Dept. of Chemistry) for the interesting and helpful analysis of my work and their attention to my progress.

This work was supported by the research grant no. 227414-04 from the Natural Sciences and Engineering Research Council of Canada (NSERC).

# Table of Contents

# List of Tables

page

# List of Figures

page

# List of Abbreviations

| | |
|---|---|
| ATP | adenosine triphosphate |
| ATPase | adenosine triphosphate synthase |
| Ec | *Escherichia coli* |
| HQNO | 2-heptyl-4-hydroxyquinoline-N-oxide |
| NADH | nicotinamide adenine dinucleotide |
| mg | milligram |
| ml | millillitre |
| mM | millmolar |
| ng | nanogram |
| NQR | $Na^+$-translocating NADH:ubiquinone oxidoreductase |
| ORF | open reading frame |
| PCR | polymerase chain reaction |
| pmf | proton-motive force |
| PMSF | phenylmethylsulfonyl flouride |
| SDS | sodium dodecyl sulphate |
| smf | sodium-motive force |
| CCCP | carbonyl cyanide-*p*-trichloromethoxypenyl hydrazone |
| Vc | *Vibrio cholerae* |
| Yp | *Yersinia pestis* |
| $\Delta$pH | transmembrane pH difference |
| $\Delta$pNa | transmembrane concentrational gradient of $Na^+$ |
| $\Delta\psi$ | transmembrane difference of electric potentials |
| $\mu$g | microgram |
| $\mu$l | microlitre |
| $\mu$M | micromolar |

# 1. INTRODUCTION AND LITERATURE REVIEW

## 1.1. Introduction: Biology and Epidemiology of *Yersinia pestis*

*Yersinia pestis* is an invasive, facultative intracellular pathogen that uses in its life cycle an arthropod vector, the flea, and a number of mammalian hosts, including humans. *Y. pestis* is a causative agent of bubonic plague, undoubtedly the most devastating bacterial infection known, with more than 200 million victims over the course of written history. The extremely high lethality of plague apparently reflects both a relatively short evolutionary history of *Y. pestis* (which diverged from the enteropathogenic *Yersinia pseudotuberculosis* within the last 20 000 years (Achtman *et al.*, 1999)) and the most unusual dissemination strategy adopted by this dangerous pathogen.

At the genetic level, rapid divergence of *Y. pestis* from *Y. pseudotuberculosis* is due to both the acquisition of certain genes by lateral transfer (on plasmids pPCP and pMT) and to the series of loss of function mutations that resulted in formation of numerous pseudogenes (Brubaker, 1991; Perry & Fetherston, 1997). In comparison to *Y. pseudotuberculosis*, *Y. pestis* lost as much as 13% of all functional genes (Chain *et al.*, 2004). Some of lost genes encode central enzymes of intermediary metabolism (such as glucose 6-phosphate dehydrogenase or aspartase); their loss is manifested in the complex nutritional requirements of *Y. pestis* (Chain *et al.*, 2004) and is related to the complex low-calcium response (see below). Products of other eliminated genes

normally provoke or potentiate inflammatory response, and their loss contributes to the acuteness of plague (Kukkonen *et al.*, 2004). Taken together, all these metabolic alterations have created and presently maintain a unique situation that favors death of the already infected animal, which compels resident fleas to leave and search for new hosts (Brubaker, 2007a). As a result, *Y. pestis* has a tightly closed flea-host-flea cycle, where bacterial dissemination only occurs in highly homeostatic environments of animal body fluids/tissues. This biochemical feature apparently makes *Y. pestis* highly sensitive to the ionic composition of its microenvironment. Another "signature" molecular aspect of the epidemiology of *Y. pestis* is its ability to bypass the immune system of the host by injecting the virulence factors directly into host cell cytoplasm via a type III protein secretion system, T3SS (Michiels *et al.*, 1990; Cornelis & Wolf-Watz, 1997; Heeseman *et al.*, 2006), whose expression appears to be both $Ca^{2+}$- and (indirectly) $Na^{+}$-sensitive (Brubaker, 2005, 2007, 2007a; Fowler *et al.*, 2009).

### 1.2. Alkali/alkaline earth metals and virulence in *Y. pestis*

As it is discussed in the following sections, one of the most curious features of the *Y. pestis* physiology and virulence is its stringent dependence upon alkali/alkaline earth cations, primarily $Na^{+}$ and $Ca^{2+}$ (Brubaker, 2005, 2007, 2007a; Fowler *et al.*, 2009). Therefore it is very important to study the transport mechanisms that regulate sodium and calcium levels in the cytoplasm of *Y. pestis*. We believe that manipulating the exchange of these cations (i.e., through the inhibition of corresponding transport systems) will provide effective means for

disruption of the infectious cycle of this dangerous pathogen, eventually yielding effective anti-bacterial remedies with completely new mechanism of action.

The lists of relevant transport systems residing in the *Y. pestis* plasma membrane are given in the following Tables 1.1and 1.2. These data were extracted from the completed genome sequence of *Y. pestis* available from the public database at http://cmr.jcvi.org.

Here, all ion transport systems listed are classified into two major categories: (1) primary pumps, that directly use metabolic energy of either oxidation of NADH (in the case of NQR (NADH:ubiquinon oxidoreductase)) or hydrolysis of ATP (in the case of Ca2+-motive ATPase) for active transport of $Na^+$ or $Ca^{2+}$, and (2) secondary pumps, that exchange these cations for protons, thus making use of the pre-established protonmotive force.

Noteworthy, two secondary cation/proton transporters, Yp-NhaP and Yp-ChaA, have both $Ca^{2+}$ and $Na^+$ ions as their substrates, as does the hypothetical $Ca^{2+}/Na^+$ exchanger Yp-YrbG. All three thus interconnect the transmembrane circulation of $Ca^{2+}$, $Na^+$ and $H^+$. Regrettably, both molecular mechanisms and physiological impact of $Na^+$ and $Ca^{2+}$ transport systems listed in Table 1 and 2 remain virtually uninvestigated. The available data on *Y. pestis* calcium and sodium transport systems or their homologues from different species are briefly discussed in the following sections.

| Table 1. Sodium transporting systems of *Y. pestis CO92* as predicted from genome analyses | | | | |
|---|---|---|---|---|
| **Locus** | **Putative function** | **Homolog** | **Similarity** | **Class** |
| YPO3235 | $Na^+$-motive NADH:quinone oxidoreductase (NQR) (multisubunit) | NqrF (*Vibrio alginolyticus*) | 88% | Primary $Na^+$ pump |
| YPO3236 | | NqrE (*Vibrio alginolyticus*) | 90% | |
| YPO3237 | | NqrD (*Vibrio alginolyticus*) | 87% | |
| YPO3238 | | NqrC (*Vibrio alginolyticus*) | 78% | |
| YPO3239 | | NqrB (*Vibrio alginolyticus*) | 86% | |
| YPO3240 | | NqrA (*Vibrio alginolyticus*) | 75% | |
| YPO0470 | $Na^+/H^+$ antiporter | NhaA (*Escherichia coli*) | 82% | Secon-dary $Na^+$ pumps |
| YPO0624 | $Na^+/H^+$ antiporter | NhaC (*Halobacterium* sp.) | 52% | |
| YPO1958 | $Ca^{2+}(Na^+)/H^+$ antiporter | ChaA (*Escherichia coli*) | 67% | |
| YPO2142 | $Na^+/H^+$ antiporter | NhaB (*Shigella flexneri*) | 87% | |
| YPO3630 | $K^+(Na^+,Ca^{2+})/H^+$ antiporter | NhaP(*Pseudomonas aeruginosa*) | 47% | |

| Table 2. Calcium transporting systems of *Y. pestis CO92* as predicted from genome analyses | | | | |
|---|---|---|---|---|
| **Locus** | **Putative function** | **Homolog** | **Similarity** | **Class** |
| YPO0451 | $Ca^{2+}$-translocating ATPase (P-type) | SP70585_1594 *(Str. pneumoniae)* | 59% | Primary $Ca^{2+}$ pump |
| YPO1958 | $Ca^{2+}(Na^+)/H^+$ antiporter | ChaA (*Escherichia coli*) | 67% | Secon-dary $Ca^{2+}$ pumps |
| YPO3576 | $Ca^{2+}/Na^+$ antiporter | YrbG (*Salmonella enterica*) | 62% | |
| YPO3630 | $K^+(Na^+,Ca^{2+})/H^+$ antiporter | NhaP(*Pseudomonas aeruginosa*) | 47% | |

### 1.3. $Na^+$ transport in *Y. pestis* and its pathogenicity

The genome of *Y. pestis* contains four ORFs encoding putative $Na^+/H^+$ antiporters: *nhaA, nhaB, nhaC* and *nhaP*. However, no analyses of these putative antiporters have been performed until recently, when Yp-NhaA has been cloned and characterized in the course of the joint project carried on in laboratories of Dr. C. Häse (Oregon State University) and Dr. P. Dibrov (University of Manitoba).

#### 1.3.1. Yp-NhaA as a major $Na^+/H^+$ exchange system

When expressed in the antiporterless strain of *E. coli* and analyzed in inside-out sub-bacterial vesicles, Yp-NhaA behaved as a typical enterobacterial $Na^+/H^+$ antiporter of NhaA type (see Padan *et al.*, 2008 for a recent review). It exchanged $Na^+$ and $Li^+$ (but not $K^+$) ions for protons in the electrogenic manner (more than 1 $H^+$ per each alkali cation) and was maximally active at alkaline pH (8.5 and higher); its apparent $K_m$ values for both substrate cations were in the low millimolar range (Winogrodzki, J. and Dibrov, P., unpublished observations). Most importantly, it has been also found that Yp-NhaA is criticial for the infectivity of *Y. pestis* (Häse, C. and Dibrov, P., personal communication). Remarkably, the *Y. pestis nhaA* deletion mutant was unable to grow in blood or serum *in vitro* (Häse, C. and Dibrov, P., personal communication).

Although the exact molecular mechanism of these defects is still under the investigation, the critical importance of Yp-NhaA for survival of *Y. pestis* in blood may have a very simple reason. It is well established that, in order to assure the

dissemination via the arthropod vector, population of *Y. pestis* must achieve a remarkably high concentration of app. $10^8$ bacteria per ml of blood in the mammalian host (Heesemann *et al.*, 2006; Brubaker, 2007a). This means that *Y. pestis* cells must be able to grow and multiply very actively in a relatively saline environment. Blood plasma normally contains from 135 to 145 mM of $Na^+$; such level of sodium is lethal for the bacteria (Padan *et al.*, 2004). On the other hand, $Na^+/H^+$ antiporters of the NhaA type are regarded as major sodium-extruding systems in enterobacteria for their ability to create and maintain large concentration gradients of $Na^+$ on the bacterial membrane (Padan *et al.*, 2001; Padan *et al.*, 2004; Padan, 2008). It could therefore be expected that elimination of Yp-NhaA would be detrimental for survival of *Y. pestis* in blood.

In addition, it has recently been demonstrated that operation of T3SS system renders cells of *Y. pestis* hypersensitive to $Na^+$, apparently elevating the cytoplasmic concentration of sodium (Brubaker, 2005, 2007; Fowler *et al.*, 2009). Thus elimination of functional Yp-NhaA must make the activation of T3SS suicidal for the bacterium.

### 1.3.2. Yp-NhaB: an auxiliary $Na^+/H^+$ antiporter?

Data on Yp-NhaB are absent in the current literature. However, based on the precedent of Yp-NhaA considered above, one could assume that in *Y. pestis* this antiporter acts similarly to its homologues from other enterobacteria.

In *E. coli*, Ec-NhaB has been extensively studied in the laboratory of Dr. E. Padan. It is an integral membrane protein of molecular weight ($M_r$) of 55,543 Da (Pinner *et al.*, 1992). Analysis of hydropathic profile predicts for Ec-NhaB 12 putative transmembrane segments linked by hydrophilic loops. In contrast to Ec-NhaA, Ec-NhaB is sensitive to amiloride, the diuretic drug that is a specific inhibitor of mammalian $Na^+/H^+$ antiporters (Pinner *et al.*, 1995). Indeed, one of transmembrane segments of Ec-NhaB contains the pentamer $^{445}$FLFLL$^{450}$, which is identical to the core of the putative amiloride-binding site of mammalian $Na^+/H^+$ antiporters (Pinner *et al.*, 1995). Ec-NhaB-catalyzed antiport is electrogenic, more than one $H^+$ being exchanged per each $Na^+$. Measured stoichiometry for Ec-NhaB is $3H^+$:$2Na^+$ (Pinner *et al.*, 1994). An important difference between Ec-NhaA and Ec-NhaB is that the activity of Ec-NhaB is modest and pH-independent. This defines Ec-NhaB as an auxiliary $Na^+/H^+$ exchanger important only when the level of NhaA activity is growth-limiting, as when cells grow at pH 6.0 or lower on the substrates that are symported with $Na^+$, such as proline, serine, or glutamate (Pinner *et al.*, 1993).

### 1.3.3. Yp-NhaC and Yp-NhaP as minor $Na^+$ extrusion systems

Because the elimination of functional Yp-NhaA results in severe hypersensitivity of the deletion mutant to external sodium (see above), one can safely assume that the contribution of Yp-NhaC and Yp-NhaP to the salt resistance (i.e., $Na^+$ ion export) in *Y. pestis* is at best very modest.

The role of Yp-NhaP as a putative "universal ion exchanger" is discussed below in the context of $Ca^{2+}$ homeostasis in *Y. pestis*. Experimental characterization of ion selectivity and transport properties of heterologously expressed Yp-NhaP is the major research objective of the present work.

### 1.3.4. Primary respiratory $Na^+$ pump, Yp-NQR

In various *Vibrio* species, active $Na^+$ extrusion occurs *via* the primary sodium pump, NADH-ubiquinone oxidoreductase, NQR (Tokuda and Unemoto, 1982; Unemoto and Hayashi, 1993; Häse and Mekalanos, 1999). Initially discovered by Tokuda and Unemoto in a free-living marine bacterium *Vibrio alginolyticus,* NQR was later found to be encoded in genomes of many Gram-negative pathogens, including *V. cholerae, Haemophilus influenzae, Klebsiella pneumoniae, Neisseria gonorrhoeae, Neisseria meningitides, Pseudomonas aeruginosa,* and *Shewanella putrefaciens* (Hayashi *et al.*, 2001). The genome of *Y. pestis* also contains a typical *nqr* operon (see Table 1). It contains six open reading frames (*nqrABCDEF*) encoding six individual subunits of the enzyme. In all characterized NQR complexes, three subunits, NqrB, NqrD, and NqrE are hydrophobic and form intramembrane core of the enzyme, while the others are more hydrophilic and protrude into the cytoplasm (Häse and Mekalanos, 1999).

While the first 5 subunits of NQR, NqrA-E, are not homologous to any proteins with known functions, NqrF is a typical redox-active protein (Hayashi *et al.*, 2001; Bogachev and Verkhovsky, 2005). Its C-terminal domain contains a

binding site for the substrate of oxidation (NADH) and site that binds FAD non-covalently; NqrF is responsible for oxidation of NADH and is called the "dehydrogenase subunit" (Bogachev and Verkhovsky, 2005). The amino acid sequence of this part of NqrF resembles ferredoxin:$NADP^+$ oxidoreductase associated with the Photosystem II in higher plants; the N-terminal domain of NqrF is homologous to ferredoxin. Therefore, the whole NqrF likely is an evolutionary product of a "fusion" of ferredoxin to ferredoxin:$NADP^+$ oxidoreductase (Bogachev and Verkhovsky, 2005). NqrF oxidizes NADH and transfers $2e^-$ to the quinone reductase, formed by subunits NqrB, D, and E (Hayashi *et al.*, 2001).

NqrB and NqrC subunits contain each one molecule of another flavin cofactor, FMN. It is covalently bound to the enzyme through a conserved threonine residue by a phosphoester bond. Such a covalent binding of flavin is unique and has been found so far only in NQR (Hayashi *et al.*, 2001). In addition to three flavin cofactors, NQR also contains one FeS-cluster (on NqrF) and one molecule of tightly bound ubiquinone-8 (Q-8), associated with the quinone reductase portion of the complex. Q-8 takes electrons from FMN and passes them to the ubiquinone of the intramembrane quinone pool thus feeding $e^-$ into the Q-cycle (Bogachev and Verkhovsky, 2005).

*In vivo* NQR oxidizes NADH and transfers two electrons to ubiquinone turning it into ubiquinol. This redox reaction is coupled to a removal of two $Na^+$ ions from the cytoplasm. Importantly, the $Na^+$ translocation results in generation

of sizable $\Delta\psi$, which was measured in direct experiments (see Unemoto and Hayashi, 1993 and references therein). This $\Delta\psi$ will prevent NQR by itself from the creation of significant $\Delta$pNa on the membrane of *Y. pestis*; the additional cation-exchanging systems, such as NhaA-type antiporter that can use $\Delta\psi$, must be involved.

Analysis of Yp-NhaA briefly mentioned above shows that the active $Na^+/H^+$ exchange mediated by this electrogenic antiporter is critical for the survival of *Y. pestis* in the host and the development of the infectious process. In contrast, deletion of the primary $Na^+$ pump, NQR, does not affect viability of *Y. pestis* (Häse, C. and Dibrov, P., personal communication).

### 1.4. $Ca^{2+}$ and virulence in *Y. pestis*

#### 1.4.1. "Low Calcium Response" (LCR) in *Y. pestis*

For a long time it has been known that *Y. pestis* is able to distinguish $Ca^{2+}$-rich extracellular host fluids from $Ca^{2+}$-poor mammalian cytoplasm (Perry & Brubaker, 1987). When the calcium level in the environment falls below ~2.5 mM, cells of *Y. pestis* growing at 37°C demonstrate a stringent "low calcium response" (LCR), manifested as an abrupt stoppage of growth accompanied by up-regulation of a type III protein secretion system, T3SS (Fowler & Brubaker, 1994; Brubaker, 2007; Fowler *et al.*, 2009). The T3SS is encoded on ~70 kb low-calcium response plasmid pCD (Hu *et al.*, 1998). It is also known as the

"enjectisome" for the direct delivery of virulence factors (Yops) into the cytoplasm of target host cell (Cheng *et al.*, 2001). $Ca^{2+}$ suppresses T3SS *via* the negative regulator YopD and associated chaperone system LcrH/SycD (Francis *et al.*, 2001).

Interestingly, the two components of LCR, i.e. bacteriostasis and up-regulation of T3SS at 37°C in a calcium-poor environment, can be dissected *in vitro* by elimination of $Na^+$ at acidic pH: under these permissive conditions cells are able to grow while expressing the full set of Yops (Brubaker, 2005, 2007). This and other observations clearly indicate that the operation of T3SS results in accumulation of toxic $Na^+$ in the cytoplasm of *Y. pestis* (Fowler *et al.*, 2009). Indeed, mutations that inactivate the T3SS-mediated secretion thus preventing the concomitant rise of intra-bacterial $Na^+$, rescue the growth at 37°C in the absence of $Ca^{2+}$ (Fowler *et al.*, 2009). *In vivo*, such interplay between T3SS-related $Na^+$ toxicity and $Ca^{2+}$ signaling should prevent export of T3SS virulence factors when bacteria are actively multiplying in $Na^+$- and $Ca^{2+}$-rich extracellular fluids, while in mammalian cytoplasm or in closed necrotic lesions, where both $[Na^+]$ and $[Ca^{2+}]$ are low, upregulated export of Yops could not harm sustained growth of the Yersinia population (Fowler *et al.*, 2009).

Thus, pioneering works of R. Brubaker and others established the central role of $Ca^{2+}$ in the timing of production of T3SS virulence factors. The most important questions arising from the intricate regulation outlined above are: What is actually sensed – $[Ca^{2+}]$ in the bacterial cytoplasm, in the periplasm, or external

[$Ca^{2+}$] in a close vicinity to the bacterial body? Is therefore $Ca^{2+}$ depletion *in vitro* mimicking contact with a target cell that could trigger T3SS secretion (Pettersson *et al.*, 1996) or is it provoking the lowering of intra-bacterial $Ca^{2+}$, which in turn modulates the regulatory T3SS circuit located in the cytoplasm (with a possible periplasmic component)? Obviously, calcium pumping directly modulates levels of $Ca^{2+}$ in all three important locations (cytoplasm, periplasm, immediate bacterial surroundings).

From this perspective, it is particularly noteworthy that the individual $Ca^{2+}$ transporters of *Y. pestis* (see Table 2), that are mediating $Ca^{2+}$ circulation in this bacterium, remain absolutely uninvestigated. Below, possible roles of these transporters in the calcium homeostasis in this pathogen are discussed.

### 1.4.2. Primary $Ca^{2+}$ pump: $Ca^{2+}$-translocating ATPase of P type

Bacterial cells usually maintain low intracellular free calcium by the operation of secondary $Ca^{2+}$ exchangers like ChaA, YrbG or NhaP. These transporters use a pre-established transmembrane gradient of another ion (typically, of proton) to remove calcium ions from the cytoplasm. Prokaryotic $Ca^{2+}$-motive ATPases appear to be rather rare. Among Gram-negative species, the first such enzyme was discovered in 1992 in *Flavobacterium odoratum*, where, surprisingly enough, it facilitated the majority of calcium transport (Gambel *et al.*, 1992). The enzyme is a typical P-type ATPase, having a phosphorylated intermediate in its catalytic cycle (hence, “P-type”). It consists of a single polypeptide, is highly sensitive to

vanadate, demonstrates an apparent $K_m$ for $Ca^{2+}$ of 2 μM, and for ATP of 130 μM, and is rapidly self-phosphorylating in a $Ca^{2+}$-dependent, vanadate-sensitive manner (Gambel *et al.*, 1992; Desrosiers *et al.*, 1996). Thus the $Ca^{2+}$-ATPase from the soil and water bacterium *F. odoratum* not only fulfills all the criteria expected of a P-type ATPase, but also shows a remarkable similarity to the eukaryotic $Ca^{2+}$-ATPase from sarcoplasmic reticulum (Gambel *et al.*, 1992).

In *Y. pestis*, the locus YPO0451 encodes a typical $Ca^{2+}$-ATPase of P type (Table 2). No experimental data on this enzyme are available at this moment, but the abovementioned precedent of *Fl. odoratum* provides a strong rationale for the future studies of physiological role and biochemical features of the $Ca^{2+}$-ATPase from *Y. pestis*.

### 1.4.3. Yp-ChaA: a standard enterobacterial $Ca^{2+}/H^+$ exchanger?

The protein encoded by YPO1958 (Table 2) is annotated as $Ca^{2+}/H^+$ (Yp-ChaA) antiporter that exhibits significant homology to ChaA of *E.coli* (Ivey *et al.*, 1993). Ec-ChaA was initially proposed to act as a specific $Ca^{2+}/H^+$ antiporter (Ivey *et al*., 1993). However, further studies have suggested its involvement in net $Na^+$ extrusion in *E. coli* (Ohyama, Igarashi, and Kobayashi 1994; Sakuma *et al*., 1998; Shijuku *et al*., 2002). Data on Yp-NhaA mentioned above suggest that Yp-ChaA hardly contributes into the overall $Na^+$ resistance of *Y. pestis*. If, unlike many

other genes in this fast-evolving pathogen, YPO1958 still encodes a functional protein, one would expect it to transport $Ca^{2+}$ ions rather than $Na^{+}$.

Widespread distribution of ChaA-type antiporters in enterobacteria implies the importance of this kind of antiporters for the $Ca^{2+}$ and $Na^{+}$ homeostasis in bacteria. It is therefore important to assess the roles of Yp-ChaA in physiology and pathogenicity of *Y. pestis* in the future studies.

### 1.4.4. Yp-YrbG resembling mammalian $Na^{+}/Ca^{2+}$ exchangers

Open reading frame located at the YPO3576 locus (see Table 2) encodes a putative $Ca^{2+}/Na^{+}$ antiporter belonging to the YRBG group of the large and diverse Cation/$Ca^{2+}$ Exchanger (CaCA) superfamily (Cai and Lytton, 2004). Despite of wealth of recently generated genomic/proteomic information (Ruknudin and Schulze, 2002; Cai and Lytton, 2004), biochemistry of this group of prokaryotic cation exchangers remains virtually unexplored experimentally. Topology of the *E. coli* homologue exhibits internal repeats of opposite orientation, but no experimental data on functioning of Ec-YrbG are available (Saaf *et al.*, 2001). The YrbG homologue from alkaliphilic *Alkalimonas amylolytica*, when expressed in antiport-deficient *E. coli*, modestly complemented $Na^{+}$ and $Ca^{2+}$ sensitivity (Wei *et al.*, 2007). In the $K^{+}$ uptake-deficient strain *E. coli*, Aa-YrbG slightly enhanced growth in the presence of limiting [$K^{+}$] (Wei *et al.*, 2007). Interestingly, the authors' attempts to demonstrate $Ca^{2+}$ or $Mg^{2+}/H^{+}$ antiport by assays previously described for cyanobacterial $Ca^{2+}/H^{+}$ antiporter (Waditee *et al.*, 2004) were negative (Wei *et*

*al.*, 2007). The authors inferred that under physiological conditions (very low levels of $Ca^{2+}$ in the environment) in the natural host, Aa-YrbG might act as a $Na^+/Ca^{2+}–K^+$ exchanger, accumulating $Ca^{2+}$ (and, perhaps, $K^+$) in exchange for cytoplasmic $Na^+$ (Wei *et al.*, 2007).

It is not clear at this moment how Yp-YrbG is contributing to the overall $Ca^{2+}$ homeostasis and virulence of *Y. pestis*; is it a $Na^+/Ca^{2+}–K^+$ or $Ca^{2+}/H^+$ antiporter.

### 1.4.5. Yp-NhaP as a putative "universal ion exchanger"

Yp-NhaP (in locus YPO3630) is a sole antiporter of NhaP-type in *Y. pestis* (Table 2). It was formally annotated as a putative $Na^+/H^+$ antiporter in the database. Its physiological significance and kinetic properties were never investigated before. Taking into account (a) a number of precedents where NhaP-type antiporters are apparently involved into the regulation of intracellular calcium levels (see Resch *et al.*, 2011 and discussion below) and (b) distribution of conserved amino acid residues in Yp-NhaP, we hypothesized that it may recognize and transport not only $Na^+$, but also $Ca^{2+}$ ions. If so, Yp-NhaP would be of a special interest, given the important role that $Na^+$ and $Ca^{2+}$ play in the physiology and pathogenicity of *Y. pestis*. We therefore decided to examine cation-transporting properties of Yp-NhaP in hope to shed a light on a possible role of in $Ca^{2+}$ homeostasis in *Y. pestis*.

Data presented in this work show that Yp-NhaP is actually the cation/proton exchanger of broad specificity, mediating $Ca^{2+}(Na^+, K^+)/H^+$ antiport in the membrane of the antiport-deficient *E. coli* strain.

### 1.5. Yp-NhaP as a member of NhaP family

#### 1.5.1. NhaP family of antiporters

The recently identified NhaP family of $Na^+/H^+$ antiporters belongs to the monovalent cation/proton antiporter CPA1 superfamily (Saier, 1999), with numerous homologues found in Gram-positive and Gram-negative bacteria, cyanobacteria, yeast, fungi, plants and animals (Fig.1.1). The history of the NhaP family started in 1998, when Utsugi and coauthors identified in *Pseudomonas aeruginosa* novel antiporter, Pa-NhaP1, that showed no homology to any bacterial $Na^+/H^+$ antiporter known at the time.

The cloned Pa-NhaP1 was expressed in its functional form in the triple *E. coli* mutant KNabc, which lacks the three major $Na^+/H^+$ antiporters (NhaA, NhaB, and ChaA) and is therefore very sensitive to environmental $Na^+$ and $Li^+$ ions. The cells of KNabc expressing Pa-NhaP1 regained normal $Na^+$ resistance, thus suggesting that the actual physiological function of Pa-NhaP1 is the removal of toxic sodium ions from the bacterial cytoplasm (Utsugi *et al*. 1998). Surprisingly, Pa-NhaP1 failed to confer to KNabc cells the resistance to $Li^+$ ions; furthermore, membrane vesicles isolated from KNabc expressing Pa-NhaP1 exhibited $Na^+/H^+$ antiport activity but no detectable $Li^+/H^+$ antiport activity (Utsugi *et al*. 1998).

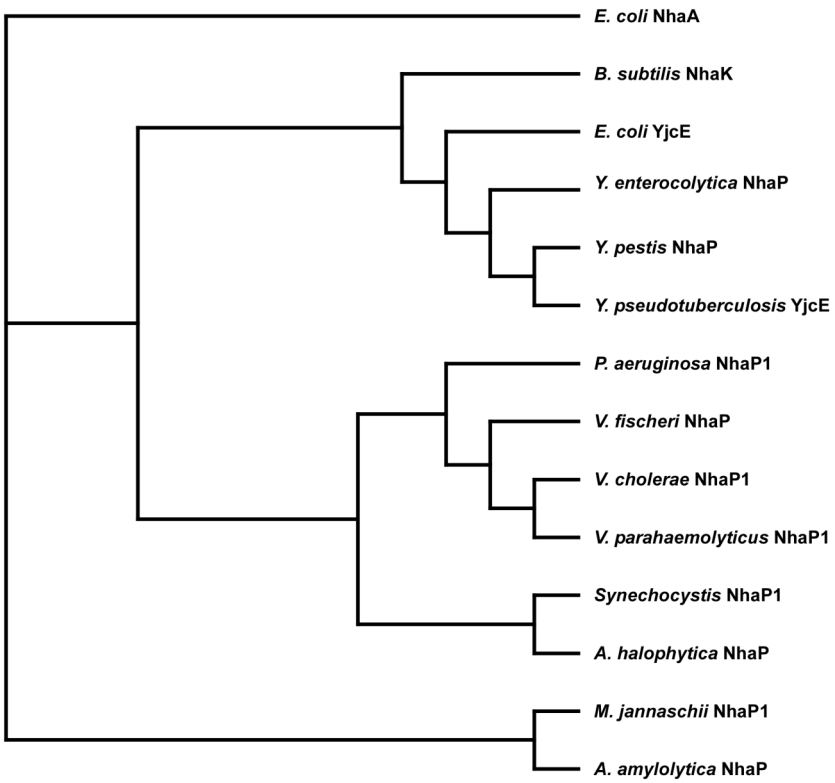


**Fig. 1.1.** Phylogenetic relationship of Yp-NhaP and various cation/$H^+$ antiporters belonging to the CPA-1 family. The sequences were aligned using ClustalW2 and the tree was drawn by TreeView. The following GenBank accession numbers refer to the cation/$H^+$ antiporters shown on the tree. *Yersinia pestis* NhaP AAM83832.1, *Yersinia pseudotuberculosis* YjCE CAH22837.1, *Yersinia enterocolitica* NhaP CAL13861.1, *Escherichia coli* YjCE ACA79563.1, *Bacillus subtilis* NhaK CAB15347.1, *Pseudomonas aeruginosa* NhaP1 AAG07048.1, *Vibrio alginolyticus* NhaP1 EEZ82069.1, *Vibrio fischeri* NhaP, *Vibrio parahaemolyticus* NhaP1, *Vibrio cholerae* NhaP1 AAF93562.1, *Synechocystis* NhaP1 BAA17925.1, *Aphanothece halophytica* NhaP BAB69459.1, *Methanococcus jannaschii* NhaP1 AAB99540.1, *Alkalimonas amylolytica* NhaP DQ649020.1. NhaA from *Escherichia coli*, whose accession number is NP_414560, was used as an out-group protein (Ap-NhaP) BAB69459.1, *V. cholerae* (Vc-NhaP3) NP_230338.1, *Synechocystis* sp. PCC 6803 (Syn-NhaP3) NP_442407.1, *Alkalimonas amylolytica* (Aa-NhaP) DQ649020.1, *Synechocystis* sp. PCC 6803 (Syn-NhaP1) NP_441245.1, *B. subtilis* (Bs-NhaG) BAA89487.1, *Staphylococcus aureus* (Sa-NhaP1) YP_499194.1, *Arabidopsis thaliana* (Ath-SOS1) NP_178307.2, *A. thaliana* (Ath-NHX8) NP_172918.1, *V. parahaemolyticus* (Vp-NhaP3) NP_799787.1, *V. vulnificus* (Vv-NhaP3) NP_933489.1, *P. aeruginosa* (Pa-NhaP3) NP_252428.1, *V. vulnificus* (Vv-NhaP1) NP_935754.1, *Agrobacterium tumefaciens* (Agt-NhaP1) NP_357539.1, *Cryptosporidium parvum* (Cp-SOS1) CAD98616.1, *E. coli* (Ec-YjcE) NP_418489.1, *P. aeruginosa* (Pa-NhaP2) NP_253708.2, *Clostridium perfringens* (Clp-NhaP2) NP_563511.1

As one can see from the Fig. 1.1, cells sometimes possess a number of NhaP paralogues. These isoforms of NhaP possibly arose as a result of gene duplication events and then evolved independently to satisfy different physiological needs in the same cell.

### 1.5.2. Cation specificity in NhaP family

The very fact of co-existence of NhaP isoforms in the same cell suggests functional diversity within this family of transporters. One would expect the two most important characteristics of antiport, its substrate specificity and pH dependence, to reflect such diversity. Table 3, based on literature data, confirms that substrate specificity is indeed very different among representatives of NhaP family. There are also some peculiarities in cation specificity that may seriously affect the physiological impact of NhaP-type cation/$H^+$ antiporters.

The first unique feature, that is shared virtually by all NhaP-type antiporters, is their ability to discriminate between $Na^+$ and $Li^+$ ions: as Table 3 shows, they all demonstrate a very poor $Li^+/H^+$ antiport (or its total absence). For all $Na^+/H^+$ antiporters characterized before Utsugi's discovery, $Li^+$ and $Na^+$ are equally good substrates (Utsugi *et al*., 1998). The usual explanation for this was based on the similarity of ion radii of both cations (0.76 Å for $Li^+$ and 1.02 Å for $Na^+$, see Murata *et al*., 2008); it was implied that proteins bind alkali cations in their de-hydrated state (Padan, 2008).

**Table 3. Substrate diversity in the NhaP family of antiporters[a]**

| Name/Organism | Substrate | pH profile |
|---|---|---|
| Mj-NhaP1/ *Methanococcus jannaschii* Hyperthermophilic archeon. in seawater (pH 4.0 to 6.0). | $Na^+$ ($Li^+$)/$H^+$ | Active at pH 7.0 and below, Blocked at pH >5.0. |
| Pa-NhaP/ *Pseudomonas aeruginosa* | $Na^+$ ($Li^+$)/$H^+$ | Sharp optimum at pH 7.5. No activity at pH 7.0 and 8.5. |
| Vp-NhaP2/ *Vibrio parahaemolyticus* | $K^+$ /$H^+$ | Active at pH 8.0 (7%) and 9(21%). |
| Aa-NhaP/*Alkalimonas amylolytic* Halotolerant, alkaliphilic | $K^+$ ($Na^+$, $NH_4^+$)/$H^+$ | Active at alkaline pH (7.0 to 9.5), Optimum is at pH 7.5 |
| Ap-NhaP1/ *Aphanothece halophytica* Halotolerant cyanobacterium. | $Na^+$ /$H^+$ at pH 5.0 to 9.0 and $Ca^{2+}$ /$H^+$ at alkaline pH (low activity). | $Na^+$ /$H^+$ antiport gradually increases from 26% (pH 5.0) to 60% (pH 9.0); $Ca^{2+}$ /$H^+$ 0% at pH 6.0, 26% at pH 7.0 |
| Syn-NhaP1 /*Synechocytis PCC 6803* | $Na^+$ ($Li^+$)/$H^+$ | High, pH-independent antiport activity at pH 5.0 to 9.0. |
| Vc-NhaP1/*Vibrio cholerae* | $K^+$ ($Na^+$)/$H^+$ | Optimum is at pH 7.75 |
| Vc-NhaP2/*Vibrio cholerae* | $K^+$ ,$Rb^+$ ,($Na^+$), $H^+$ | Optimum is at pH 7.75 |
| Vc-NhaP3/*Vibrio cholerae* | $K^+$ /$H^+$ | Optimum is at pH 7.75 |

In the light of this explanation, inability of Pa-NhaP1 to transport $Li^+$ looks puzzling. Moreover, some NhaP-type antiporters transport both $Na^+$ and $Li^+$. For example, Syn-NhaP1 from the cyanobacterium *Synechocystis* PCC 6803 complemented both $Na^+$-sensitivity and $Li^+$-sensitivity in *E. coli* TO114 (triple antiporter mutant similar to KNabc) and showed similar $Na^+/H^+$ and $Li^+/H^+$ antiport activities when assayed in the TO114 sub-bacterial vesicles (Hamada *et al*., 2001; Waditee *et al*., 2001). Syn-NhaP1 was also able to mediate $Ca^+/H^+$ but not $K^+/H^+$ exchange (Hamada *et al*., 2001; Waditee *et al*., 2001). $Ca^{2+}$ also is a substrate for Ap-NhaP, the $Na^+/H^+$ antiporter from the halotolerant cyanobacterium *Aphanothece halophytica* (Waditee *et al*., 2001, 2004). It could be mentioned here that the well-studied Ec-NhaA does not transport $K^+$ (Padan *et al*., 2004; Padan, 2008) but, when reconstituted into proteoliposomes, mediate not only $Na^+(Li^+)/H^+$ exchange, but also $Ca^{2+}/H^+$ exchange (Dibrov, 1993).

Recently, it has been suggested that all these data related to cation specificity, including the seemingly contradictory case of $Li^+$, could be explained by a simple "size-exclusion principle" (Resch *et al.*, 2011). The authors pointed out that the radii of dehydrated ions are increasing in order $Li^+$(076 Å) < $Ca^{2+}$(0.99 Å) < $Na^+$(1.02 Å) < $K^+$(1.38 Å), and the ion-binding cavities in Syn-NhaP1 or NhaA might be too small to accommodate a bulky $K^+$ ion. This principle provides a simple explanation to a well-known fact that many $Na^+/H^+$ antiporters discriminate $K^+$ ions – they apparently have small ion-binding pockets. On the other hand, they should be able to accommodate smaller cations, such as $Ca^{2+}$ and $Li^+$.

Furthermore, according to this logic all $K^+/H^+$ antiporters should have the most spacious ion-binding pockets and thus they should be able to bind all smaller cations including $Li^+$ and $Na^+$.

But how to explain that small $Li^+$ ion is a poor substrate for many NhaP-type antiporters or that Vc-NhaP3 acts as a specific $K^+/H^+$ antiporter, discriminating all smaller ions (see Table 3)? Based on their results concerning the cation specificity in Vc-NhaP2 (Resch *et al.*, 2010), Resch and co-authors suggested "ligand shading" as a mechanism that may diminish or even completely prevent $Na^+(Li^+)/H^+$ *exchange* (but not $Na^+$ or $Li^+$ *binding*) in some antiporters possessing large ion-binding pockets (Resch *et al.*, 2011). They found that that $Li^+$ competes with $K^+$ for binding to Vc-NhaP2. Moreover, Vc-NhaP2 was able to exchange $Li^+$ for $K^+$, but it failed to catalyze $Li^+/H^+$ antiport (Resch *et al*., 2010). It should be mentioned here that in $Na^+/H^+$ antiporters all substrate cations and protons compete for binding to the protein. This was demonstrated experimentally (see, for example, Dzioba-Winogrodzki *et al*., 2009) and inferred from structural data (Padan, 2008). Generalized catalytic cycle of a $Na^+/H^+$ antiporter is presented in Fig. 1.2. $C_o$ and $C_i$ are conformations with the ion-binding site accessible from the outer medium or from the cytoplasm, respectively. Reorientation of unloaded carrier, or slippage ($C_o \leftrightarrow C_i$) is prohibited, because it would result in proton uniport and total de-energization of the membrane. Only one alkali cation, $Na^+$, is shown for simplicity. Note that, in addition to the cation/$H^+$ antiport, "heterologous" $Na^+/Ca^{2+}$ antiport is possible (along the pathway $5 \leftrightarrow 6 \leftrightarrow 7 \leftrightarrow 8 \leftrightarrow 9 \leftrightarrow 10$).

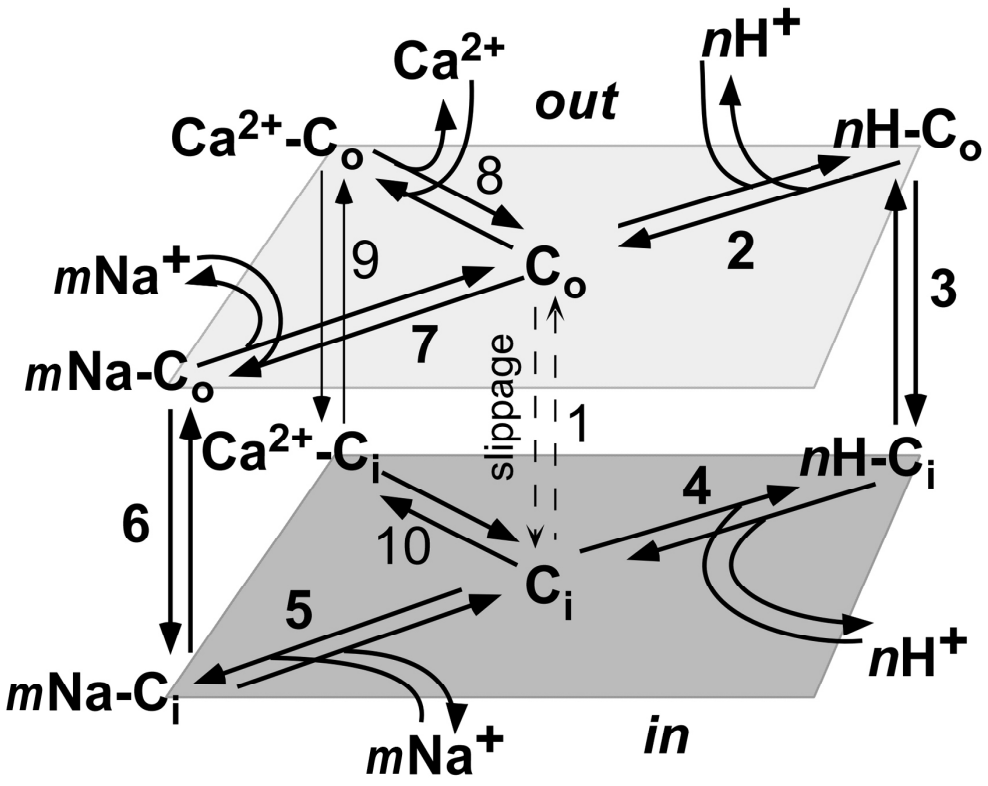


**Fig.1.2.** Generalized catalytic cycle of a $Na^+/H^+$ antiporter that can also transport $Ca^{2+}$. $C_o$ and $C_i$ are conformations with the ion-binding site accessible from the outer medium or from the cytoplasm, respectively. Reorientation of unloaded carrier ($C_o \leftrightarrow C_i$) is prohibited, because it would result in proton uniport and total de-energization of the membrane. Only one alkali cation, $Na^+$, is shown for simplicity. In addition to the "regular" cation/$H^+$ exchange along the pathways 2→3→4→5→6→7 and 2→3→4→10→9→8, so-called "heterologous" $Na^+/Ca^{2+}$ antiport is possible (along the pathway 5↔6↔7↔8↔9↔10). In the case of an electroneutral antiport, there must be $m$=$n$; note that it does not mean that $m$=$n$=1 (i.e.,that the *actual* stoichiometry of the exchange is equal to the *minimal* one). In particular, when $n$=$m$=2, any mode of ion antiport mediated by the antiporter will be electroneutral.

According to the idea of “ligand shading”, in the cases similar to Vc-NhaP2, all the substrate ions bind to the different subsets of ligands available within the spacious cation-binding site. If these ligand subsets are overlapping, substrate ions will directly compete with one another for common ligands. While $H^+$ requires only one electronegative ligand, the optimal number for coordination of $Na^+$ ion by polypeptides is six (Glusker *et al*., 1999). Authors further suggest that the “normal” $Li^+/H^+$ exchange (but not binding of $Li^+$ to the antiporter) will be prevented if the $Li^+$ ion uses the same ligand as $H^+$, because $H^+$ (a single coordination bond) will be unable to displace $Li^+$ (six coordination bonds). Apparently, $Li^+$ could prevent the $H^+$ binding indirectly (“ligand shading”), as well (Resch *et al.*, 2011). On the other hand, $Na^+$ or $K^+$ could bind to different ligands that do not include the ligand for $H^+$. Since both alkali cations normally form 6 to 8 coordination bonds with proteins (Glusker *et al*., 1999), unlike protons, they should easily displace $Li^+$ from the ion-binding pocket. This would make possible “heterologous” $Na^+/Li^+$, $Ca^{2+}/Na^+$, or $K^+/Li^+$ exchange, as well as the regular exchange of both $Na^+$ and $K^+$ with protons, but not $Li^+/H^+$ exchange (see Fig.1.2). Such “heterologous” exchange by Vc-NhaP2 was indeed reported in (Resch *et al*. 2010). Noteworthly, having nearly identical affinities for $K^+$ and $Na^+$, the Vc-NhaP2 easily exchanged $K^+$ for $H^+$, but was unable to catalyze $Na^+/H^+$ antiport (Resch *et al*., 2010). This also could be explained by “ligand shading”, if binding of $Na^+$ to Vc-NhaP2 results in a “partial shading”, that is if it does not prevent the protonation of the proton-binding ligand completely, but makes it less efficient (Resch *et al.*, 2011).

Summing this part up, one can say that the idea of “ligand shading” together with the “size-exclusion principle” explain all the experimental data concerning diverse ion specificity in the NhaP family summarized in Table 3. The ability of some NhaP-type antiporters to transport $Ca^{2+}$ (see Tabl. 3), considered together with apparently minor contribution of Yp-NhaP into salt resistance of *Y. pestis* (see the above sections), indicates the intriguing possibility that Yp-NhaP could act as a $Ca^{2+}/H^+$ or possibly $Ca^{2+}/Na^+$ antiporter rather than $Na^+/H^+$ antiporter *in vivo*.

### 1.5.3. The pH profiles of activity in NhaP family

Available data on the pH-dependence of NhaP-type antiporters are presented in the third column of Table. 3 As one can see, there are significant variations in their pH ranges and pH optima. The two antiporters discussed above, Syn-NhaP1 and Ap-NhaP1, maintain high activity in the entire range from pH 5.0 to pH 9.0 (Waditee *et al.*, 2001). Other antiporters of NhaP type have pH-optima at different points. Thus, Vc-NhaP2 is inactive at pH 6.5 and pH 9.5, and shows the optimum of activity at pH about 7.8 (Resch *et al.*, 2010). Not surprisingly, in more alkalitolerant organisms such optima are shifted towards higher pH values. Aa-NhaP from alkaliphilic bacterium *Alkalimonas amylolytica* N10 has an optimum for $K^+/H^+$ transport at pH 8.0 and still demonstrates significant activity at pH 9.5 (Wei *et al.*, 2007). In contrast, Mj-NhaP1 from the hyperthermophilic archaeon *Methanococcus jannaschii*, which grows optimally at

85°C, has a narrow “window of activity” between pH 6.0 and 7.0 (Hellmer *et al*., 2002).

Being under such a tight pH-control, Mj-NhaP1 is thought to fine-tune the internal pH. In *M. jannaschii*, the cytoplasmic pH is maintained around 6.5. If the internal pH rises or lowers slightly, Mj-NhaP either pumps $H^+$ in, while extruding $Na^+$, or pumps $H^+$ out using the existing $Na^+$ gradient, respectively. However, if pH fluctuations are more extreme, the antiporter must be switched off to prevent uncontrolled $Na^+$ accumulation or cytoplasmic acidification (Vinothkumar *et al.*, 2005). According to the data of electron cryo-microscopy, a certain central part of Mj-NhaP responds to the pH-shifts away from 6.0 by a 2Å swing. This is thought to reflect “open” (i.e., active) and “closed” (inactive) conformations of the antiporter. (Vinothkumar *et al.*, 2005). Vinothkumar and co-authors suggests that the pH changes would lead to protonation-deprotonation of the negatively charged side chains of a specific small set of residues, thus inducing conformational changes resulting in the activation or inactivation of the transporter (Vinothkumar *et al.*, 2005). Of note, this mechanism of pH regulation was originally suggested for the major enterobacterial $Na^+/H^+$ antiporter, Ec-NhaA (see Hunte *et al.*, 2005; Padan, 2008).

Determination of pH-profile of the activity of Yp-NhaP is one of the objectives of the present work.

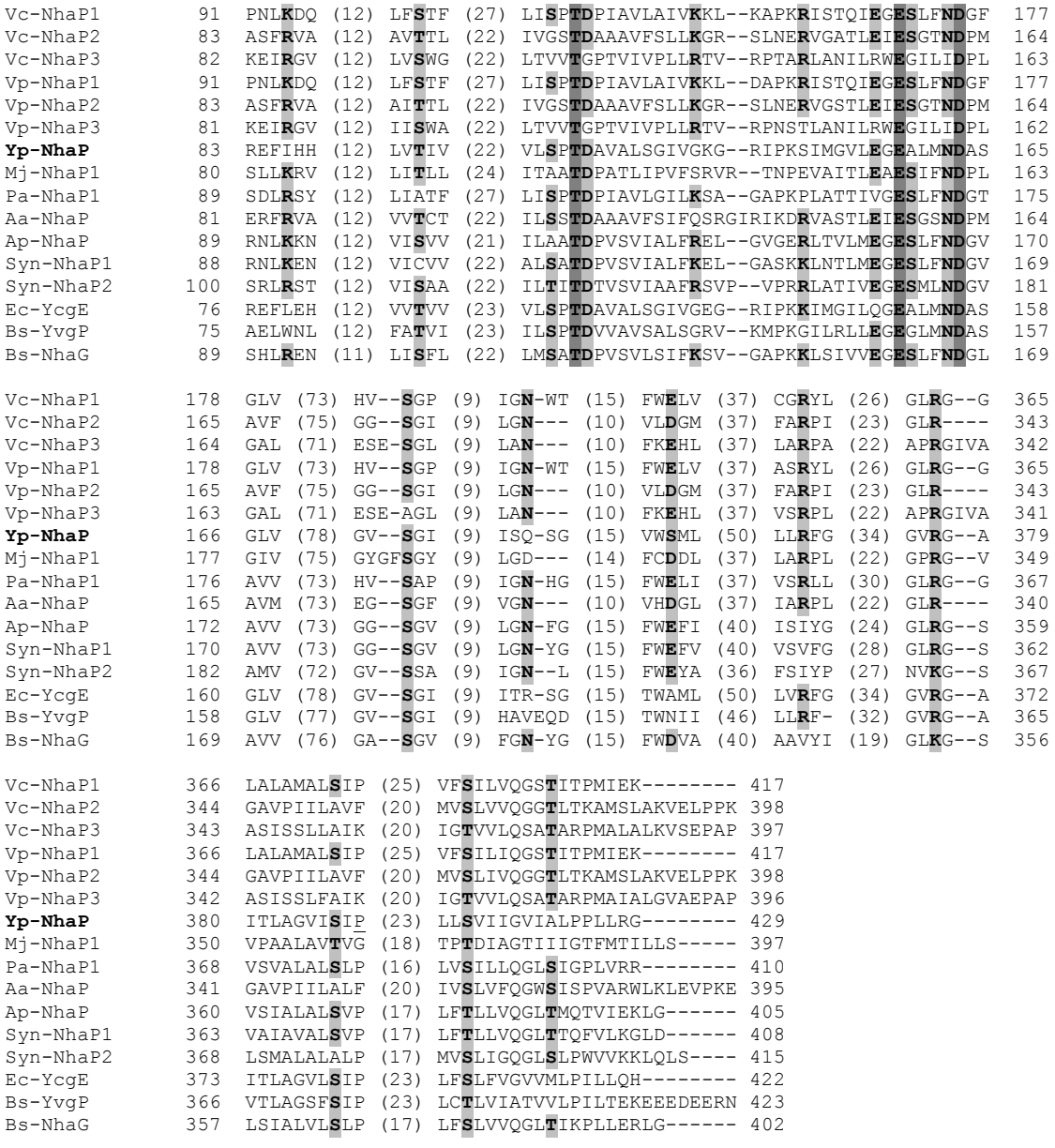


**Fig. 1.3.** Multiple alignment of partial sequences members of the NhaP family showing conserved amino acid residues that might be involved in the cation binding, together with their close neighbors. Shadowed are the most conserved residues associated with transmembrane segments. See the text for more discussion (After Resch *et al.*, 2011, with minor modifications).

### 1.5.4. Conseravative amino acid residues in Yp-NhaP

A multiple partial alignment of the members of the NhaP family is presented in Fig. 1.3. (taken from Resch et *al.*, 2011, with modifications). It reveals a number of highly conserved residues associated with hydrophobic transmembrane segments. From their number, negatively charged ones are of a special interest, because they could form part of the cation-binding pocket by providing their side chains as cation-coordinating ligands. Several conserved aspartate residues have been targeted for mutagenesis in different laboratories. In Syn-NhaP1, replacement of Asp138 with Glu or Tyr completely abolished both $Na^+/H^+$ and $Li^+/H^+$ antiport activity (Hamada *et al*., 2001). In Mj-NhaP1, the aspartate residue in the same position (D132 in Mj-NhaP1) as well as D161 were found to be critical for the antiport activity (Hellmer *et al*., 2003). It is possible that these negatively charged side chains of these conserved residues serve as ion-coordinating ligands for translocated cations. (In Fig. 1.3, these residues are shown as D133 and D162, respectively, following the enumeration of residues in Vc-NhaP2.) Other highly conserved charged or polar residues that might be of importance are T132, E157, N161, S245, N259, R315, R343 and S/T376 (Fig. 1.3).

Of note, two NhaP-type antiporters that have been demonstrated to transport $Ca^{2+}$ among other substrate cations, namely Ap-NhaP1 and Syn-NhaP1, which, as well as Yp-NhaP, all have a positively charged arginine in position 83 (in the Yp-NhaP enumeration, see Fig. 1.3). This might indicate that Yp-NhaP

also has calcium ion as its substrate. The present work was designed to check this exciting possibility. Arginine in the same conserved position (R76) is also present in Ec-YcgE, a putative cation-proton antiporter that is phylogenetically close to the sub-cluster of NhaP3 orthologues from the genus *Vibrio* (see Fig. 1.1). To the best of our knowledge, cation selectivity of this transporter still awaits its investigation. Interestingly, a positive charge in the same conserved position in the form of lysine could be seen in NhaP3 orthologues from *Vibrio* species, as well. Vc-NhaP3 from *Vibrio cholerae* was recently cloned in our laboratory, and its cation specificity is currently under investigation.

### 1.5.5. Deduced topology of Yp-NhaP

Structure of antiporters belonging to the NhaP family seems to be as diverse as their functional properties. Especially diverse are eukaryotic NhaP proteins. They vary in size more than twice (from 500 to >1000 residues). For example, SOS1 from *Arabidopsis thaliana*, one of the first $Na^+/H^+$ antiporters found in higher plants, has 1146 amino acids (Shi *et al*., 2000). The body of the protein consists of the two distinct parts: hydrophobic membrane module of 12 transmembrane segments and long hydrophilic C-terminus exposed to the cytoplasm (Shi *et al*., 2000; Pardo *et al*., 2006). Prokaryotic NhaPs are typically smaller with approximately 550 amino acids, but they also have integral membrane modules and hydrophilic C-termini protruding into the cytoplasm.

The deduced topology of Yp-NhaP is presented in Fig. 1.4.

**A** **TMHMM predicted topology**

```
# Sequence Length: 556
# Sequence Number of predicted TMHs:  11
# Sequence Exp number of AAs in TMHs: 242.25569
# Sequence Exp number, first 60 AAs:  31.58499
# Sequence Total prob of N-in:        0.31015
# Sequence POSSIBLE N-term signal sequence

Sequence TMHMM2.0 outside       1     9
Sequence TMHMM2.0 TMhelix      10    27
Sequence TMHMM2.0 inside       28    92
Sequence TMHMM2.0 TMhelix      93   115
Sequence TMHMM2.0 outside     116   119
Sequence TMHMM2.0 TMhelix     120   142
Sequence TMHMM2.0 inside      143   167
Sequence TMHMM2.0 TMhelix     168   190
Sequence TMHMM2.0 outside     191   194
Sequence TMHMM2.0 TMhelix     195   214
Sequence TMHMM2.0 inside      215   225
Sequence TMHMM2.0 TMhelix     226   243
Sequence TMHMM2.0 outside     244   247
Sequence TMHMM2.0 TMhelix     248   270
Sequence TMHMM2.0 inside      271   282
Sequence TMHMM2.0 TMhelix     283   305
Sequence TMHMM2.0 outside     306   319
Sequence TMHMM2.0 TMhelix     320   342
Sequence TMHMM2.0 inside      343   367
Sequence TMHMM2.0 TMhelix     368   390
Sequence TMHMM2.0 outside     391   404
Sequence TMHMM2.0 TMhelix     405   427
Sequence TMHMM2.0 inside      428   556
```

**B**

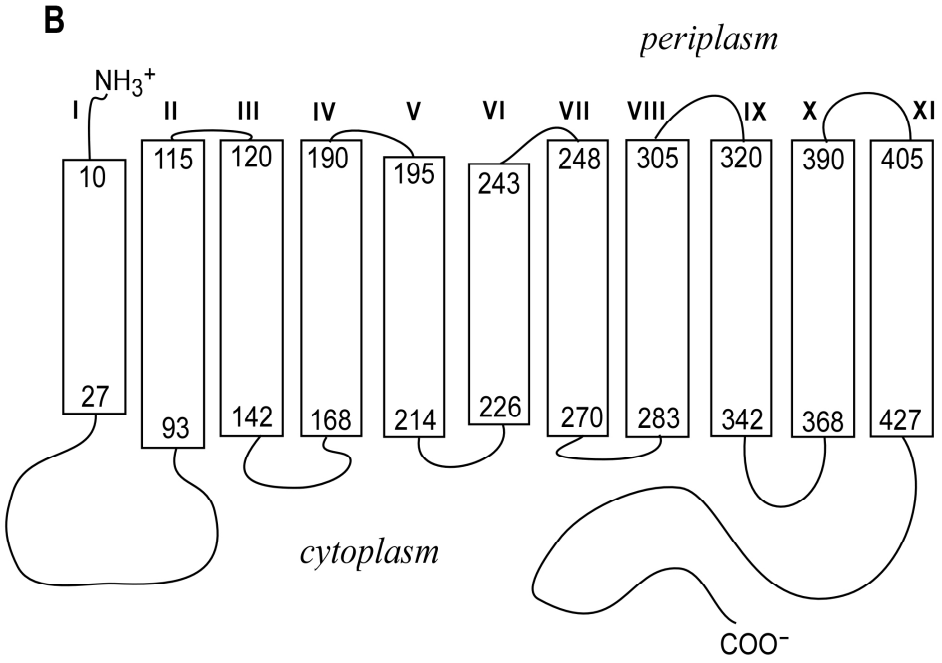


**Fig. 1.4.** Deduced topology of Yp-NhaP. This topology was produced using TMHMM program available at public domain http://www.cbs.dtu.dk/services/TMHMM-2.0.
**A**: The TMHMM run results. **B**: Graphic representation of the deduced Yp-NhaP topology.

As one can see, Yp-NhaP displays an architecture that is typical for NhaP-type proteins with an integral membrane module of 11 transmembrane segments and an extended cytoplasmic C-terminus.

### 1.6. Hypothesis and Research Objectives

**Hypothesis:** Taking into account (*a*) a number of precedents where NhaP-type antiporters are apparently involved into the regulation of intracellular calcium levels and (*b*) distribution of conserved amino acid residues in Yp-NhaP (in particular, the presence of Arg in the conserved position 83), we hypothesized that not only $Na^+$, but also $Ca^{2+}$ ion may be a substrate for Yp-NhaP.

Specific **research objectives** of this work are:

1) Cloning and functional expression of Yp-NhaP in the antiport-deficient strain of *E. coli* TO114.

2) Examination of the cation specificity of Yp-NhaP in the experimental model of inside-out membrane vesicles produced from the cells TO114 expressing Yp-NhaP.

3) Determination of apparent $K_m$ values for each substrate cation.

4) Determination of pH-profiles of activity of Yp-NhaP for each transported cation.

5) Probing the stoichiometry of ion exchange mediated by Yp-NhaP by registration of $\Delta\psi$ changes with the fluorescent potential-sensitive dye, Oxonol V.

6) Investigation of possible physiological role of Yp-NhaP by systematic comparison of growth properties of the chromosomal deletion *Yp-nhaP* mutant of *Y. pestis*, its isogenic wild-type parent, and the deletion mutant expressing Yp-NhaP *in trans*.

## 2. MATERIALS AND METHODS

### 2.1. Bacterial Strains and Plasmids.

*Yersinia pestis* strains used in this project are KIM5.3001 (Δ*pgm*) and its derivative with the *Yp-nhaP* gene deleted, KIM5.3001(Δ Δ*nhaP*). KIM strains used in this study are pigmentation minus (Pgm$^-$) strains that are avirulent (Une and Brubaker, 1984). Pgm$^-$ strains carry a deletion of a 102-kb region of the genome. These strains are attenuated due to loss of the *pgm*-encoded yersiniabactin siderophore-based iron transport system (Bearden *et al*., 1997). The Δ*pgm* strains therefore are heavily attenuated and not pose any health hazard to the personnel. These strains were kindly provided by Dr. C. C. Häse (Oregon State University).

For the functional expression of the cloned Yp-NhaP, we used the $Na^+/H^+$ antiporter-deficient strain of *E. coli* TO114 (F 1 IN (*rrnD-rrnE*) *nhaA*::$Km^R$ *nhaB*::$Em^R$ *chaA*::$Cm^R$), which was kindly provided by Dr. T. Nakamura (Niigata University of Pharmacy and Applied Life Sciences, Niigata, Japan).

For cloning and plasmid construction, DH5α (*supE*44 *hsdR*17 *recA*1 *endA*1, *gyrA*96 *thi*-1 *relA*1) (US Biochemical Corporation) or TOP10 ($F^-$ *mcr*A Δ(*mrr-hsd*RMS-*mcr*BC) φ80*lacZ*ΔM15 Δ*lac*X74 *rec*A1 *ara*D139 Δ(*ara leu*) 7697 *gal*U *gal*K *rps*L ($Str^R$) *end*A1 *nup*G) (Invitrogen) were used as hosts.

Plasmid that was used in cloning of Yp-*nhaP* gene was the commercial expression vector pBAD24 (Invitrogen). The map of pBAD24 is shown in Fig. 2.1.

## 2.2. Bacterial Culture Conditions.

The basic growth media used for the cultivation of bacteria and growth experiments were:

**Undefined Rich Media:**

**LB Broth (per litre)**

**10 g Bacto-Tryptone**
**5 g Yeast Extract**
**5 g Sodium Chloride (NaCl)**

**LBK Broth (per litre)**

**10 g Bacto-Tryptone**
**5 g Yeast Extract**
**5 g Potassium Chloride (KCl)**

**LBB Broth (per litre)**

**10 g Bacto-Tryptone**
**5 g Yeast Extract**

**Blood Base Broth (per litre)**

**10 g Beef Extract**
**10 g Peptone**
**5 g Sodium Chloride (NaCl)**

**Non-Cationic Adjusted Blood Base Broth (per litre)**

**10 g Meat Extract**
**10 g Peptone**

**Defined Medium**

**56.4 g 5x M9 Minimal Salts**

Formulation (per litre):

| | |
|---|---|
| **33.9 g** | **Sodium Phosphate, Dibasic** |
| **15 g** | **Potassium Phosphate, Monobasic** |
| **2.5 g** | **Sodium Chloride (NaCl)** |
| **5 g** | **Ammonium Chloride** |

**Synthetic Medium for *Y. pestis* (sodium-free):**

The following 2× stock solution of amino acids was prepared and autoclaved:

| | |
|---|---|
| **9.0 mM** | **DL-alanine** |
| **7.6 mM** | **L-isoleucine** |
| **4.0 mM** | **L-leucine** |
| **3.2 mM** | **L-methionine** |
| **4.8 mM** | **L-phenylalanine** |
| **2.8 mM** | **L-threonine** |
| **13.6 mM** | **L-valine** |
| **2.0 mM** | **L-arginine-HCl** |
| **14.0 mM** | **L-proline** |
| **2.2 mM** | **L-lysine-HCl** |
| **5.2 mM** | **L-glycine** |
| **2.2 mM** | **L-tyrosine** |

Salt Solution (10× stock) was filter sterilized and stored at 4ºC before use:

| | |
|---|---|
| **Citric Acid** | **0.1M** |
| **Magnesium Oxide** | **0.2M** |
| **$FeSO_4$** | **1.0 mM (from 100× stock solution)** |
| **$MnSO_4$** | **0.1 mM (from 100× stock solution** |

Potassium Phosphate Solution (100× stock) was prepared separately, filter sterilized and stored at 4ºC:

| | |
|---|---|
| **$K_2HPO_4$** | **0.25 mM** |

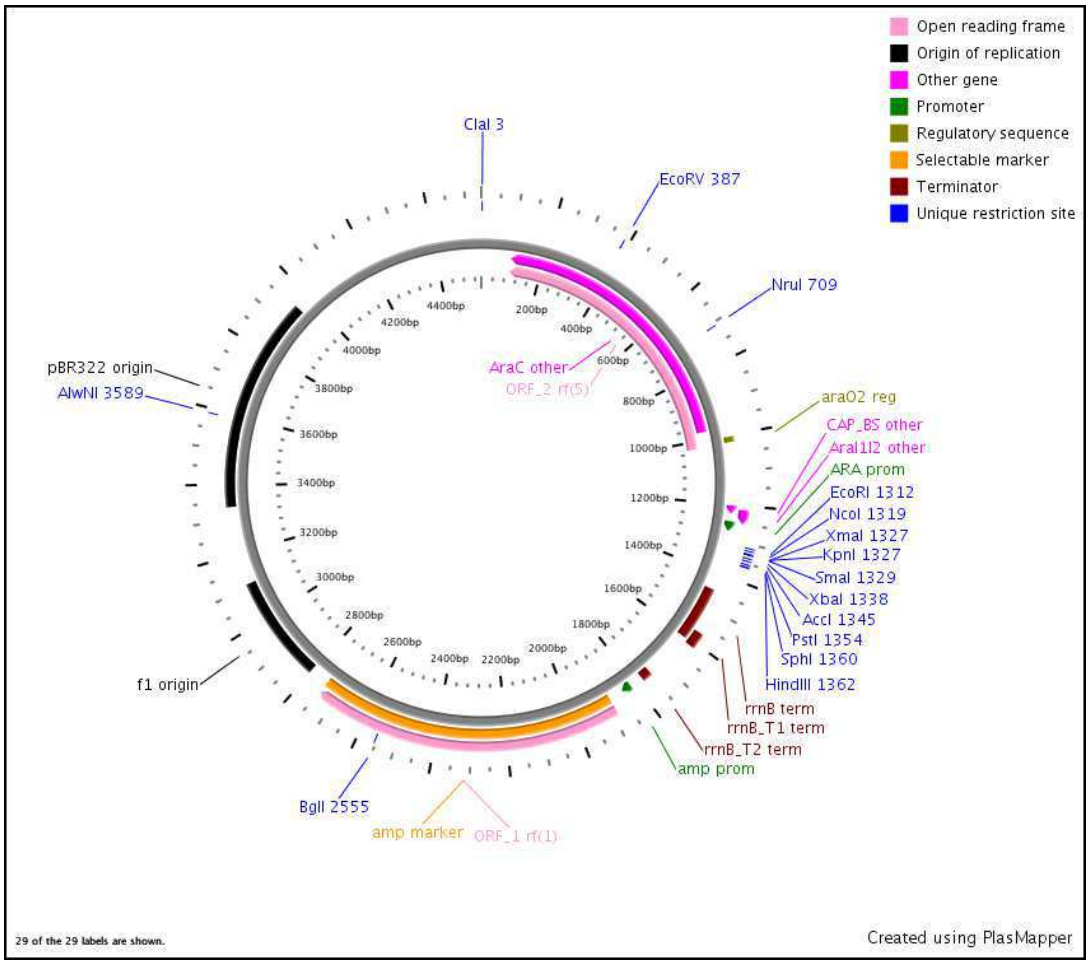


**Fig. 2.1.** Genetic map of the expression vector pBAD24 (Invitrogen) used in this work. As created by: http://en.bio-soft.net/plasmid.html
http://wishart.biology.ualberta.ca/plasmapper/

The separate components were mixed and supplemented with antibiotics as needed prior to the inoculation of bacteria. Antibiotics were prepared and stored as the following stock solutions:

***Ampicillin (100 mg/ml):*** 1 gm of ampicillin was placed into a 15 ml Falcon tube. 10 ml of double distilled water was added and vortex until mixed. The solution was filter sterilized into a fresh tube. Aliquots of 1 ml were placed in microtube, and Stored at –20$^{o}$C.

***Kanamycin (30 mg/ml):*** 300 mg of kanamycin were placed into a 15 ml Falcon tube. 10 ml of double distilled water was added and vortex until mixed. The solution was filter sterilized into a fresh tube. Aliquots of 1 ml were placed in Eppendorf tube, and Stored at –20$^{o}$C.

***Chloramphenicol (34 mg/ml):*** 340 mg of chloramphenicol were placed into a 15 ml Falcon tube. 10 ml of 95% ethanol were added and vortex until mixed. Aliquots of 1 ml were placed in Eppendorf tube, and Stored at –20$^{o}$C.

***Erythromycin (100 mg/ml):*** 1 gm of erythromycin was placed into a 15 ml Falcon tube. 10 ml of 95% ethanol were added and vortex until mixed. Aliquots of 1 ml were placed in Eppendorf tube, and Stored at –20$^{o}$C.

***Streptomycin (100 mg/ml):*** 1 gm of streptomycin was placed into a 15 ml Falcon tube. 10 ml of double distilled water was added and vortex until mixed. The solution was filter sterilized into a fresh tube. Aliquots of 1 ml were placed in Eppendorf tube, and Stored at –20$^{o}$C.

Well-isolated single colonies of *Y. pestis* were picked up from agar and propagated on fresh 1.5% agar plates containing the appropriate antibiotics. Overnight growth was typically conducted at 28$^{o}$C (or other growth temperature as indicated). The streaked plates were kept at 4$^{o}$C for up to seven days, and used as a source of inoculum for the overnight cultures. After seven days, fresh plates were streaked-out from glycerol stocks. If growth experiments were carried out with single colonies, fresh plates were streaked out from the above plate for every growth experiment.

For the preparation of overnight cultures, a test-tube with 3.0 ml of liquid medium containing the appropriate antibiotics was inoculated with a pool of three to four separate colonies, three to four parallels for each test strain. The inoculum was grown for 16-18 hours overnight (*Y. pestis* overnights must be twice-cultivated in test medium prior to growth experimentation) at 28$^{o}$C (or other growth temperature as indicated).

In a typical growth experiment, three to four parallels were set up for each strain under given conditions. Bacterial growth was monitored as turbidity of culture at 600 nm, and data were plotted using the Excel program (Microsoft).

Conditions for growth of *E. coli* are described in the corresponding sections below.

## 2.3. Cloning and Expression of Yp-NhaP

### 2.3.1. Isolation of Chromosomal DNA from *Y.pestis*

Chromosomal DNA from *Y.pestis* KIM5.3001 strain was isolated according to the following protocol: Overnight cultures were prepared in liquid medium (6.0 ml per test tube for a single prep) containing ampicillin (100 mg/ml). Cultures were grown overnight at 28$^{o}$C. Then 1.5 ml of bacterial culture was put into Eppendorf tubes and pelleted in a microcentrifuge set at high-speed (14,000 rpm) for two minutes. Supernatant was removed by aspiration.

200 μl of Lysis Buffer (containing 40 mM Trizma base, 20 mM sodium acetate, 1mM EDTA, 1% SDS) was added to each pellet. Then pellets were resuspended completely by vigorous pipetting.

20 μl of 10 mg/ml RNase solution was added to the suspension. Then preparations were incubated at 37ºC for 45 minutes.

10μl of 4M NaCl was added to each preparation and mixed well. To remove cellular debris, mixtures were centrifuged at maximum speed in a microcentrifuge (14,000 rpm) for 30 minutes. Each supernatant was carefully decanted into fresh Eppendorf tube.

DNA was extracted by adding 300 μl of chloroform to each tube. Solutions were mixed gently by inverting the tubes 50 times to get a milky solution. Then they were centrifuged at 14,000 rpm for three minutes. Upper layer was transferred with a pipette into a new Eppendorf tube.

The chromosomal DNA was precipitated by adding 700 μl of ice-cold 95% ethanol followed by spinning at maximum speed in a microcentrifuge (14,000 rpm) for 15 minutes. Ethanol was removed by aspiration.

DNA pellets were washed once with 500 μl of ice-cold 70% ethanol. Then the pellets were dried on the bench for 20-30 minutes and resuspended in 50-100 μl of TE buffer.

### 2.3.2. PCR Amplification of *Yp-nhaP* Gene

The putative ORF encoding Yp-NhaP was cloned by high-fidelity PCR, using chromosomal DNA isolated from *Y.pestis* KIM5.3001 cells as described above, with the oligonucleotide primers that introduce two unique restriction sites, with sticky ends and compatible with unique cutting sites in the polylinker of pBAD24. The PCR was done using “Fusion” high fidelity enzyme (Invitrogen). The primers were:

Forward primer: 5’ GATCACAGAATTCTGTCATGTGGAG 3’, to introduce cutting site for *Eco*RI;

Reverse primer: 5’ CCGTAAGCTTTTAACCTTCTTTTTC 3’, to introduce cutting site for *Hind*III.

Small aliquots of each PCR products were subjected to the electophoresis in 1% agarose gel, to confirm the existence of the products, and the size of the

desired fragment. 300 μl of PCR products were accumulated, and then run on 1% agarose gel, and the band of interest was immediatly cut out. DNA was extracted using QIAQuick kit according to the manufacturer's protocol. The extracted DNA was digested using EcoRI and HindIII and purified using Magnetswitch kit (Invitrogen) according to the manufacturer's (Quiagen) protocol.

### 2.3.3. Vector Preparation

pBAD24 was isolated from *E.coli* strain DH5α using a standard Alkaline Mini protocol:

Overnight cultures were prepared in liquid medium containing the appropriate selectable markers (6.0 ml/test tube for a single prep). Cultures were grown overnight at 37$^{o}$C. 1.5 ml of bacterial culture was put into 10 Eppendorf tubes and pelleted in a microcentrifuge at high-speed (14,000 rpm) for two minutes. Supernatant was removed by aspiration. 200 μl of Resuspension Buffer (containing 50 mM glucose, 10 mM EDTA, 25 mM Tris, pH adjusted to 8.0 with HCl) was added to each pellet, in addition to and 10 μl of 10 mg/ml RNase solution. Then pellets were resuspended completely by pipetting up and down with a pipette. 300 μl of Lysis Buffer (containing 0.2M NaOH and 1% SDS) was added to each tube, and mixed by inverting five times. Then tubes were incubated at room temperature for five minutes. 300 μl of Neutralization Buffer (containing

3M potassium acetate, pH adjusted to 4.8 with glacial acetic acid) was added and mixed by inverting five times. Then tubes were incubated at room temperature for five minutes.

Tubes were centrifuged at 14,000 rpm for 15 minutes, and then the supernatant was transferred to a new Eppendorf tube. 10 μl of 10 mg/ml RNase solution was added to each tube followed by incubation at 37$^{o}$C for 45 minutes. DNA was extracted by adding 450 μl of chloroform to each tube, followed by centrifugation at 14,000 rpm for three minutes, then upper layer in each tube was drawn off with a pipette into fresh Eppendorf tubes.

The plasmid DNA was then precipitated by adding 700 μl of ice-cold 95% ethanol followed by spinning at maximum speed in a microcentrifuge (14,000 rpm) for 15 minutes. Ethanol was removed by aspiration. Then the DNA pellets were washed once with 500 μl of ice-cold 70% ethanol, dried on the bench for 20-30 minutes and resuspended in 50-100 μl of TE buffer.

The isolated plasmid was digested by *Eco*RI and *Hind*III, and 300 μl of digested plasmid were de-phosphorylated using Antarctic Shrimp Phosphatase (New England labs). Following the electrophoresis in 1% agarose gel, the band of interest was cut out and the digested vector was extracted using QIAQuick kit according to the manufacturer's protocol (Quiagen).

### 2.3.4. Ligation and Clone Selection

Ligation was done using recombinant ligase enzyme from Fermentas, with the Insert:Vector ratio 4 to 1 (vol/vol), with adding sterile water instead of insert in the control tube. DH5α competent cells were transformed with both the ligation product and the control, and then plated on LB medium containing Ampicillin (100 mg/ml).

After the overnight incubation at 37ºC, 18 single Amp-resistant colonies were picked up and propagated each in 50 ml of LB supplemented with 100 μg/ml of ampicillin. Plasmid DNA was isolated from each culture as described above, and resuspended in 100 μl of TE buffer. 10 μl-aliquots were digested with the combination of *Eco*RI and *Hind*III and examined by electrophoresis in 1% agarose gel. One sample of successful ligation (see "Results and Discussion") was chosen for the further work. Selected clone was used to isolate ultra-pure DNA by Alkaline Miniprep protocol, and the isolated DNA was sent for sequencing to the University of Calgary DNA Core Unit.

### 2.3.5. Preparation of Chemically Competent *E. coli* Cells

Overnight cultures were prepared by inoculating 3.0-5.0 ml of liquid medium (typically LB or LBK) containing the appropriate antibiotics. Growth was done at 37$^{o}$C for 16-18 hours.

Overnight culture was diluted 1/500 into two 250 ml Erlenmeyer flasks containing each 40 ml of liquid medium (typically LB or LBK) as well as the appropriate antibiotics. Cells were grown at 37$^{o}$C with vigorous aeration (orbital shaker at 250 rpm) until mid-logarithmic phase ($OD_{600}$ = 0.5-0.6). When growth was completed, the cultures were chilled on ice for 20 minutes.

Chilled cells were transferred aseptically to clean, sterile 50 ml centrifuge tubes. Tubes were balanced and the cells were pelleted in a centrifuge at 12,000 rpm for 10 minutes.

The supernatant was removed by careful aspiration. Aseptically 10 ml of 0.1 M $CaCl_2$ (ice-cold) was added and cell pellets were re-suspended by pipetting up and down with a 10 ml pipette.

Tubes were placed on ice for 10 minutes, and then centrifuged for 10 minutes at 12,000 rpm. Supernatant was discarded by careful aspiration. Aseptically 10 ml of 0.1 M $CaCl_2$ (ice-cold) was added and re-suspended by pipetting up and down with a 10 ml pipette.

Tubes were placed on ice for 30 minutes, and then centrifuged for 10 minutes at 12,000 rpm.

Cell pellet was re-suspended in approximately 1/50th the original volume in 0.1 M $CaCl_2$ containing 16% glycerol (ice-cold) and stored at –80ºC up to 3 month.

### 2.3.6. Transformation of T0114 *E. coli* with the pYp-NhaP

10-20 μl of plasmid DNA were aliquoted into a sterile Eppendorf tube. Then 100 μl of chemically competent cells were added to the tube and mixed by pipetting up and down. The mixture was incubated on ice for 30-45 minutes.

Heat-shock was applied to the cells for 90 seconds at 42$^{o}$C in the heat-block. After that, cells were incubated on ice for 5 minutes. Then cells were allowed to recover by adding 1.0 ml of liquid medium (typically LB or LBK plus antibiotics to select for only and no other antibiotics [plasmid markers]) at 37$^{o}$C for 45 minutes to one hour. After recovery cells were pelleted in a microcentrifuge (14,000 rpm) for two minutes. The pellet was resuspended in 100 μl liquid LB or LBK medium. Suspension was spread onto LB or LBK agar plates containing the appropriate antibiotics.

The streaked plates were incubated overnight at 37$^{o}$C. Next day well-isolated colonies were picked up and inoculated in LBK medium supplemented with the appropriate antibiotics. The inoculum was incubated at 37$^{o}$C aerobically. Vigorous aeration was achieved by shaking at 250 rpm. Next day aliquots were prepared from the inoculum and stored as glycerol stocks (1 ml of bacterial culture mixed with 0.5 ml of 50% glycerol) at -80$^{o}$C.

## 2.4. Analysis of Growth Phenotype of the Chromosomal NhaP-deletion Mutant.

Three strains used were *Yersinia pestis* KIM5.3001 (wild type), *Y. pestis* KIM5.3001 with *Yp-nhaP* chromosomal deletion, and the same mutant transformed with pYp-NhaP plasmid expressing the *Yp-nhaP* gene for complementation trials).

The four studied cations ($K^+$, $Na^+$, $Li^+$, $Ca^{2+}$) were added to the growth media as chloride salts in increased concentrations: $1\times10^{-3}$M, $1\times10^{-2}$M, $1\times10^{-1}$M, 0.2M, 0.3M, 0.4M, 0.45M, 0.5M, 0.55M, 0.6M.

Four parallel cultures were set up from overnight starters in 3.0 ml of synthetic media in the presence of 100 μg/ml streptomycin, the tubes were grown at 28ºC overnight (18 hours) with shaking (250 rpm). The next morning, the turbidity was checked at 600 nm ($OD_{600}$).

Electrocompetent cells of *Y. pestis* were prepared as follows:

Overnight cultures were prepared by inoculating 3.0-5.0 ml of liquid medium (typically LB or LBK) containing 100 μg/ml streptomycin. The inoculum was grown at 28°C for 16-18 hours. Next day overnight culture was diluted 1/50 into a two 250 ml Erlenmeyer flasks containing 40 ml of liquid medium (typically LB or LBK) with the appropriate selectable markers. Cells were grown at 28°C, 250 rpm until mid-logarithmic phase ($OD_{600}$ = 0.8-1.0). Hourly readings were taken. When

growth was complete, the cultures were chilled on ice for 20 minutes. Then cells were transferred aseptically to clean, sterile 50 ml centrifuge tubes and pelleted in Beckman centrifuge at 12,000 rpm for 10 minutes. Supernatant was discarded by careful aspiration. The pellets were suspended in 10 ml of double-distilled water (ice-cold), by pipetting up and down with a 10 ml-pipette. The suspension was centrifuged again at 12,000 rpm for 20 minutes. Pellets were resuspended in 10 ml of YPT Buffer (ice-cold) and centrifuged once more at 12,000 rpm for 20 minutes. Finally, cells were re-suspended in approximately 1/100th of the original volume using YPT Buffer (ice-cold), and aliquoted 100 μl into sterile Eppendorf tubes. Tubes were flash-frozen in liquid nitrogen, and stored at –80$^{o}$C.

The electrocompetent cells of *Y. pestis* were electroporated with the pYp-NhaP construct. 5 μl of purified DNA were aliquoted on ice (re-suspended in sterile double-distilled water) into a sterile Eppendorf tube. 100 μl of electrocompetent cells were added to the tube and mixed by pipetting up and down. DNA-cell mixture was put into an ice-chilled 0.2 cm-gapped electroporation cuvette, and the suspension was tapped down. Electroporation was carried out using the following parameters: 2.5 kV at 5.0 milliseconds using Biorad MicroPulser. Immediately after electroporation, 1.0 ml of liquid medium (typically LB or LBK containing 100 μg/ml streptomycin) was added and mixed by pipetting up and down. The suspension was transferred to a clean, sterile test-tube. Another 1.0 ml of liquid medium was added. The suspension was incubated at

37°C for two hours before plating on LBK plates with the same concentration of streptomycin.

**2.5. Isolation of the Inside-out Sub-bacterial Membrane Vesicles.**

Four 2L-flasks were prepared containing one litre of LBB each. Then they were autoclaved. When the medium had cooled, appropriate antibiotics were added (30 μg/ml kanamycin, 34 μg/ml chloramphenicol, 100 μg/ml erythromycin, 100 μg/ml ampicillin) to each flask. The flasks were stored at 4°C prior use no longer than 1 week.

For each isolation of vesicles, eight 5.0 ml overnight cultures were prepared: four of TO114/pBAD24, and four of TO114/pYp-NhaP. They were prepared in LBK containing 30 μg/ml kanamycin, 34 μg/ml chloramphenicol, 100 μg/ml erythromycin, 100 μg/ml ampicillin. The eight tubes were grown at 37°C for 16-18 hours. Then each 2L flask was inoculated with two overnight starter cultures. The flasks were incubated at 37°C with shaking at 250 rpm, and the bacterial growth was monitored till the late logarithmic phase (four to six hours). Then the expression of Yp-NhaP was induced by adding 0.05 % (w) of arabinose. Hourly readings were taken. Growth was monitored until the $OD_{600}$ reached approximately 1.2. Then cells were pelleted by centrifugation at approximately 9,000 rpm at 4ºC for 10 minutes using three 250 ml centrifuge bottles per two litres of culture. Collected cells were washed once and concentrated down to two 250 ml centrifuge bottles with ice-cold “Krulwich” Buffer (140 mM choline chloride,

20mM Tris , and 10% glycerol) as follows: First, 50 ml of buffer was added to one of the cell pellets and it was resuspended by a pipette. Then the suspension was transferred to the second cell pellet and re-suspended. The resulted suspension was transferred to the third pellet and re-suspended. Half of the suspension (25 ml) was transferred into one of the previous 250 ml centrifuge bottles, and then 100 ml of buffer were added to each bottle and swirled to mix (two bottles final for each strain). The resulting cultures were centrifuged for 10 minutes at approximately 9,000 rpm at 4$^{o}$C. Supernatant was discarded, and pellet was re-suspended in 25 ml of ice-cold "Krulwich" Buffer. 25 ml of buffer were added to each bottle and mixed thoroughly. Bottles were cetrifuged for 10 minutes at approximately 9,000 rpm at 4$^{o}$C. After the final wash step, supernatant was discarded and each cell pellet was resuspended in 20 ml of ice-cold "Krulwich" Buffer. A mixture of protease inhibitors was combined and added to the cells as follows: 20 μl 1M DTT (final concentration 1μM), 20 μl 1 mg/ml pepstatin-A (final concentration 1 μg/ml) and 20 μl 100mM PMSF (final concentration 100μM). A small scoopful (5 mg) of DNase (Sigma$^{R}$) powder was added as well and the mixture swirl to mix.

Cells were disrupted by passing them through the French Press at 4$^{o}$C, ~20,000 psi ("1000" on the scale, MED ratio) two times. During the second passage, cells were pressed into 50 ml centrifuge bottles. The unbroken cells were pelleted at 14,000 rpm for 20 minutes at 4$^{o}$C. The supernatant was transferred into ultracentrifuge bottles, and the volume of each was adjusted to

50ml by adding “Krulwich” Buffer containing the protease inhibitor mixtures which was mentioned above, then the resulted suspension was ultracentrifuged in a Ti70 rotor at 4$^{o}$C for 1.5 hours at 50,000 rpm. Supernatant was discarded carefully, and a small volume was left behind for re-suspension. Membranes were re suspended using small-gauged needles attached to a syringe, and aliquoted into Eppendorf tubes. Eppendorf tubes were flash-frozen in liquid nitrogen and stored at –80$^{o}$C.

### 2.6. Assays of Proton-Antiporter Activity: Measurement of Transmembrane pH Gradient, ΔpH.

The activity of recombinant Yp-NhaP in inside-out membrane vesicles was registered by measuring the changes in the fluorescence of weak penetrating amine, Acridine Orange (AO). The principle of this method is illustrated in Fig. 2.2. Neutral but not ionized form of AO can penetrate the vesicles membranes by diffusion. Since Acridin Orange emits light upon illumination (fluorescence), uptake of AO by energized vesicles results in quenching of its fluorescence. In our experiments, 10 mM D-lactate was used to energize the vesicles. Added D-lactate was oxidized by the lactate dehydrogenase (LDH) that is located on the inner face of the cytoplasmic membrane. This oxidation results in the development of an electrochemical proton gradient across the membrane, which can be used for oxidative phosphorylation (respiration), and for active transport. When inside-out vesicles are energized by respiration in cation-free medium, $H^{+}$ is pumped into the vesicle interior, resulting in formation of ΔpH (acid inside) and in

the uptake of AO, registered as fluorescence declining (quenching). After addition of the studied cation, cation/$H^+$ exchange leads the efflux of AO, and as a result the fluorescence rises (de-quenching), and new steady state emerges. The ratio of de-quenching to the lactate-induced quenching of the AO fluorescence is the measure of antiport activity. In this work, the antiport activities were expressed as percent restoration of lactate-induced fluorescence quenching.

For experiments with *E.coli* vesicles, a series of experemintal buffers were prepared with varying pHs (6.0, 6.5, 7.0, 7.5, 8.0, 8.5, 9.0), using HCl to adjust pH. 2.0 ml of "Krulwich" Analysis Buffer (140mM choline chloride, 50mM Bis-Tris-Propane adjusted to desired pH, 5mM $MgCl_2$, and 10% glycerol) was put into a standard cuvette with 10mM high path, then an aliquot of vesicles equivalent to 200 μg of membrane protein and 4 μl of 8mM acridine orange were added. The cuvette was placed in Shimadzu RF-1501 spectrofluorometer (Shimadzu Scientific Instruments Incorporated). The scan was started using the excitation light at 492.0 nm, and the AO fluorescence was followed at 528.0 nm for approximately 30 seconds until a steady-level was achieved. Then 10 mM D-lactate was added as 20μl of 1M stock solution. The respiration-dependent generation of ΔpH was followed until a new steady-state of AO fluorescence was achieved. After that, the studied cation was added as a chloride salt at the indicated concentration. The addition was made as 10 μl of an appropriate stock solution prepared on the experimental buffer used. The resulting dissipation of ΔpH was followed until a new steady-state was reached.

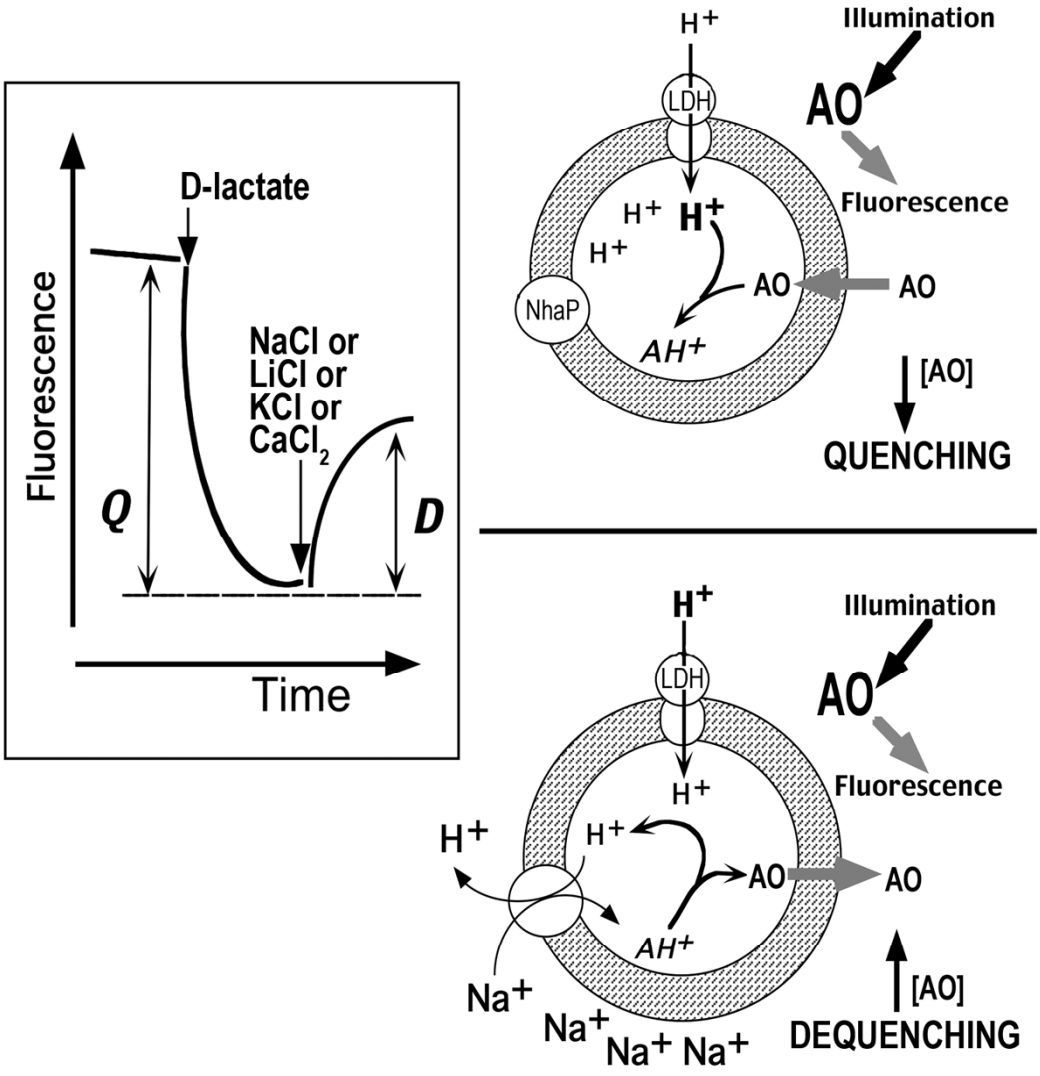


**Fig. 2.2.** Measurement of the cation/$H^+$ antiport activity in inside-out membrane vesicles by the Acridine Orange fluorescence dequenching. See the text for details.

## 2.7. Measurement of Transmembrane Difference of Electric Potentials, $\Delta\psi$.

Measurements of $\Delta\psi$ were performed on Shimadzu RF-1501 spectrofluorometer with the anionic dye Oxonol V (bis[3-phenyl-5-oxoisoxazol4-yl]pentametheneoxonol) instead of AO essentially as described above with the following modifications. Excitation light was at 595.0 nm, and emission light was monitored at 630.0 nm. To prevent collapse of $\Delta\psi$ by chloride, choline-Cl in "Krulwich" buffer was replaced by 280 mM sorbitol. 20 mM Trisma Base (pH 8.0) was used instead of BTP. To collapse unwanted $\Delta$pH and thus maximize $\Delta\psi$, 20 mM diethanolamine (pH 8.0) was added just before vesicles. The studied cations were added at indicated final concentrations as sulfates except for $Ca^{2+}$, which was added as gluconate. As a standard control, at the end of each experiment, 10 $\mu$M CCCP was added to collapse $\Delta\psi$ completely.

## 2.8. Protein Determination.

Protein content in preparations of isolated sub-bacterial vesicles was measured with the DC Protein Assay Kit (purchased from Bio-Rad), according to the manufacturer's instructions for membrane proteins.

## 2.9. Computer Analysis of Amino Acid Sequences and Kinetic Parameters.

Deduced topology of Yp-NhaP was produced using TMHMM program available at public domain http://www.cbs.dtu.dk/services/TMHMM-2.0.

Apparent $K_m$ values for different substrate cations were determined using the PRISM™ software (purchased from GraphPad Software, Inc., La Jolla, CA 92037 USA). The same software was used to plot the activity of Yp-NhaP as a function of the concentration of each probe cation.

## 2.10. Materials.

All chemicals used for this project were purchased from either Sigma-Aldrich or Fisher Scientific and were of highest purity grade available. Restriction endonucleases and other DNA-modifying enzymes were purchased from Invitrogen, Fermentas or New England Biolabs. Acridine Orange was purchased from Fluka Biochemika.

## 3. RESULTS AND DISCUSSION

### 3.1. Cloning of *Yp-nhaP* gene

The putative open reading frame (size of 1671bp) encoding Yp-NhaP was cloned by high-fidelity PCR as described in Materials and Methods, using chromosomal DNA isolated from *Y.pestis* KIM5.3001, with oligonucleotide primers that introduce two unique restriction sites (for EcoRI and HindIII) compatible with unique cutting sites in the polylinker of pBAD24 (see Fig. 2.1). The high fidelity of PCR was achieved by using Eppendorf$^{R}$ mastercycler machine, and "Fusion" DNA polymerase (Invitrogen), thus minimizing the possibility of mismatches during the reaction.

Figure 3.1 shows the results of the PCR reaction at different concentrations of chromosomal DNA template. We found that excess of the template significantly reduced the yield of the PCR reaction (Fig. 3.1, panel **a**). After a number of trials and errors, the optimal conditions for PCR reaction were found, including dilution of chromosomal DNA template (0.20 ng of DNA per reaction, which corresponds to the 1:100 dilution of the original DNA template stock solution) and addition of 2 μM DMSO to the reaction mixture (Fig. 3.1, panel **b**).

PCR product was separated from the template, concatemeric forms of fragment and excess of primers by the electrophoresis in 1% agarose gel, and the

band of product was immediately cut out from the gel under a low-intensity UV-illumination. Then DNA was extracted with QIAQuick kit, digested by EcoRI and HindIII and finally purified using Magnetswitch kit.

The cloning vector pBAD24 was also digested with the same enzymes (see Fig. 3.2A) and purified from the gel. Purified vector and insert (Fig. 3.2B) were ligated as described in Materials and Methods and used to transform competent cells of *E. coli* DH5$\alpha$. After the overnight incubation at 37ºC, 15 out of 18 well-isolated $Amp^R$-colonies were picked up, numbered and propagated in liquid medium for the isolation of plasmid DNA. Isolated plasmid DNA was used for the restriction analysis of individual clones.

Results of the restriction analysis of the selected transformant clones are shown in Figure 3.3. Aliquotes of isolated plasmid DNA were subjected to the digestion with the enzymes used for construction, i.e. EcoRI and HindIII. By doing this, we automatically checked that the sequence in the area of these restriction sites is not damaged in the process of ligation. Although a number of clones showed the expected restriction pattern of 3992 kb vector plus 1.680 kb insert (see Fig. 3.3), plasmid DNA preparations of only two clones, #9 and #10, were sent for DNA sequencing to the DNA Sequencing Facility at the University of Calgary in order to check the fidelity of construction. DNA sequence of the whole insert in the plasmid from clone # 9 was found to be identical to the published sequence, so clone #9 was selected for the further work. Plasmid DNA isolated from this clone was used to transform *E. coli* TO114 cells.

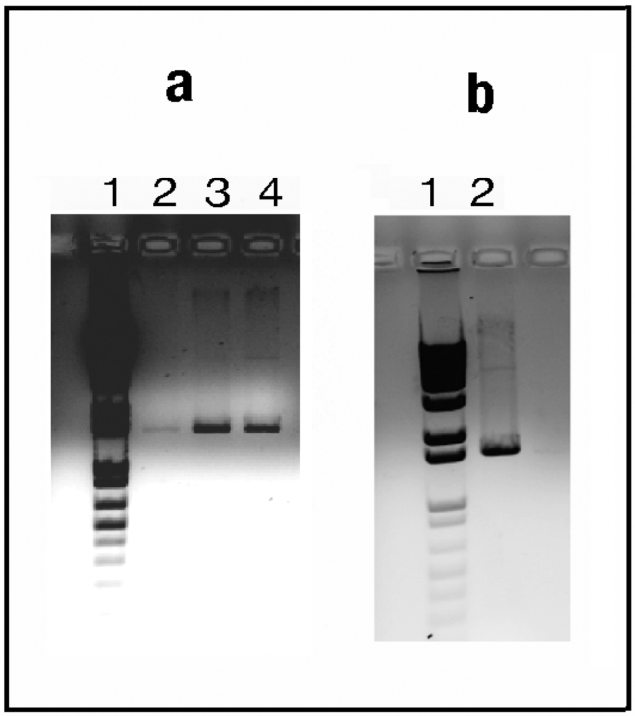


**Fig. 3.1.** Amplification of the 1.692 kb fragment that contains the *Yp-nhaP* gene at different dilution of the chromosomal DNA of *Y.pestis*. **a:** Line 1:1kb-ladder, line 2: 20.0 ng DNA per reaction; line 3: 0.2 ng DNA per reaction; line 4: 0.1 ng DNA per reaction A; **b:** 0.2 ng DNA per reaction plus 2 μM DMSO added to the reaction mixture.

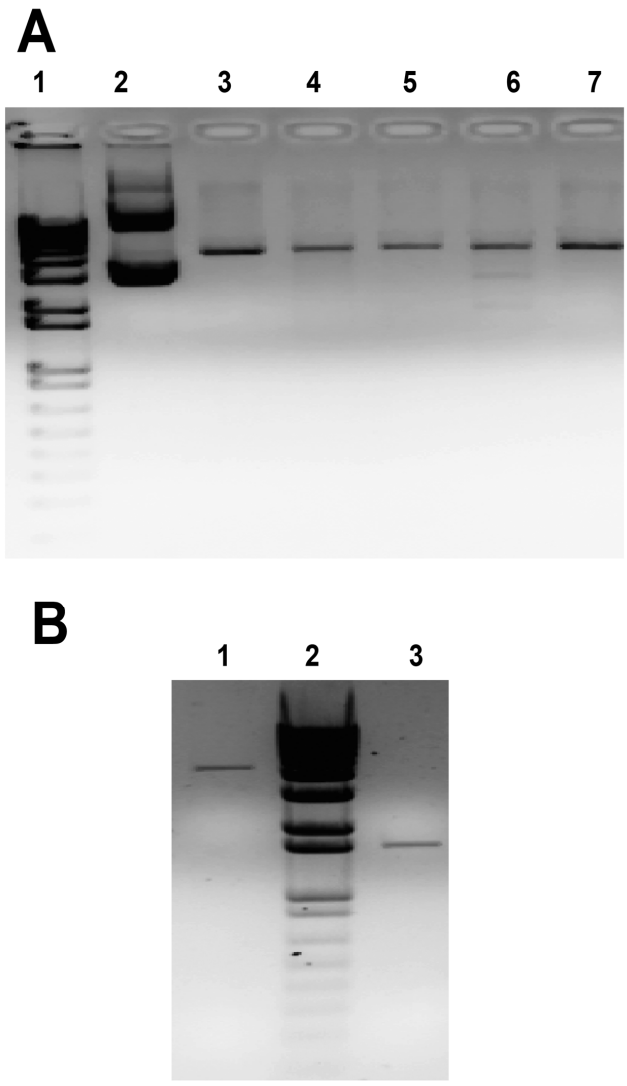


**Fig. 3.2.** Details of the cloning of *Yp-nhaP* into pBAD24. **A**: Restriction of pBAD24 with EcoR1& HindIII. Line 1: 1kb ladder; Line 2: intact pBAD24; Line 3: pBAD24 digested with EcoR1; Line 4: pBAD24 digested with HindIII(NEL)$^{R}$; Line 5: pBAD24 digested with HindIII (Invitrogen)$^{R}$; Line 6: pBAD24 digested with EcoR1 plus HindIII (NEL)$^{R}$; Line 7: pBAD24 digested with EcoR1 plus HindIII (Invitrogen). **B**: Test agarose gel of vector (3992 kb, line 1) and the insert (1.680 kb, line 3) after purification.

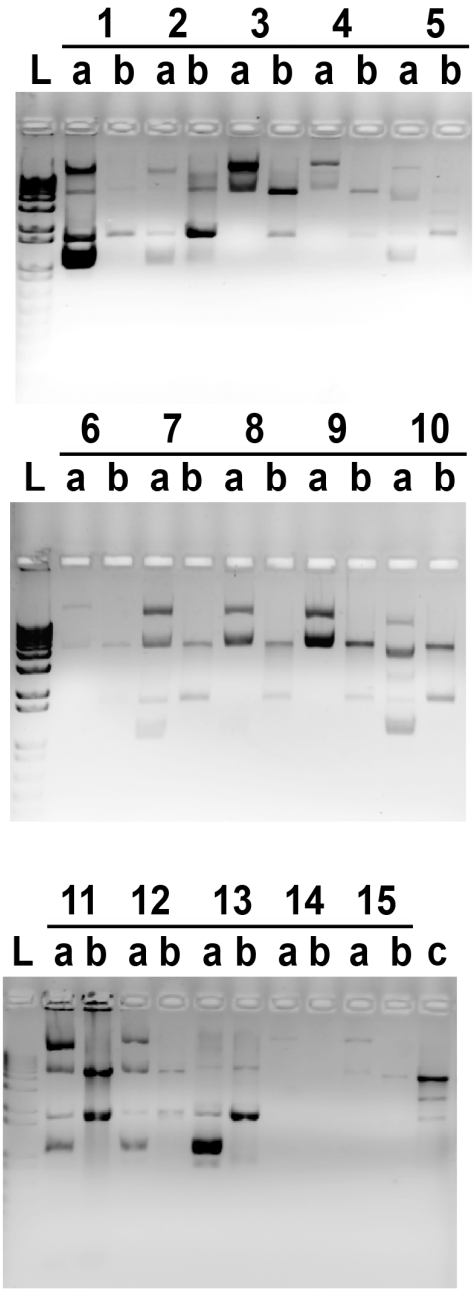


**Fig. 3.3.** The restriction analysis of 15 obtained transformant clones. Plasmid isolated from each clone was digested with the restriction enzymes used for construction and analyzed by electrophoresis in 1% agarose gel. For each clone, "a" is undigested construct, "b" is digested construct. "L" – 1kb DNA Ladder; "c" – partial digestion of "empty" pBAD24. Clone # 9 was chosen for the functional expression of Yp-NhaP (after verification of the fidelity of the construct by DNA sequencing).

## 3.2. Cation selectivity of Yp-NhaP expressed in *E. coli*

### 3.2.1. Broad cation specificity of Yp-NhaP

The very first antiport activity assays in sub-bacterial vesicles obtained from TO114 cells expressing Yp-NhaP *in trans* revealed that Yp-NhaP has a broad selectivity toward translocated cations (Fig. 3.4). When assayed with 10 mM of probe cation at pH 8.0, Yp-NhaP showed the ability to exchange protons for alkali cations $Na^+$, $Li^+$ and $K^+$, as well as for divalent $Ca^{2+}$ (Fig. 3.4). Typically, the dequenching of AO fluorescence in response to the addition of $Na^+$ and $K^+$ to the lactate-energized vesicles at this pH was quite robust (slightly higher than 30%), while for $Li^+$ and $Ca^{2+}$ it was somewhat lower (about 20%). The pH value of 8.0 was chosen for these ion specificity assays because it is close to the optimal for the activity for Yp-NhaP with $Li^+$ and $Ca^{2+}$ (see Fig. 3.9).

The ability of Yp-NhaP to catalyze $Ca^{2+}/H^+$ antiport makes it similar to two other proteins of the same family, Syn-NhaP1 and Yp-NhaP. This experimental observation supports our working hypothesis that a positively charged arginine in position 83 (in the Yp-NhaP enumeration, see Fig. 1.3) might be a structural predictor of the ability of an antiporter of NhaP type to use calcium ion as a substrate. It will be interesting to check experimentally whether another positively charged residue, lysine, found in the same position in Vc-NhaP3 and its close isoforms plays an analogous role.

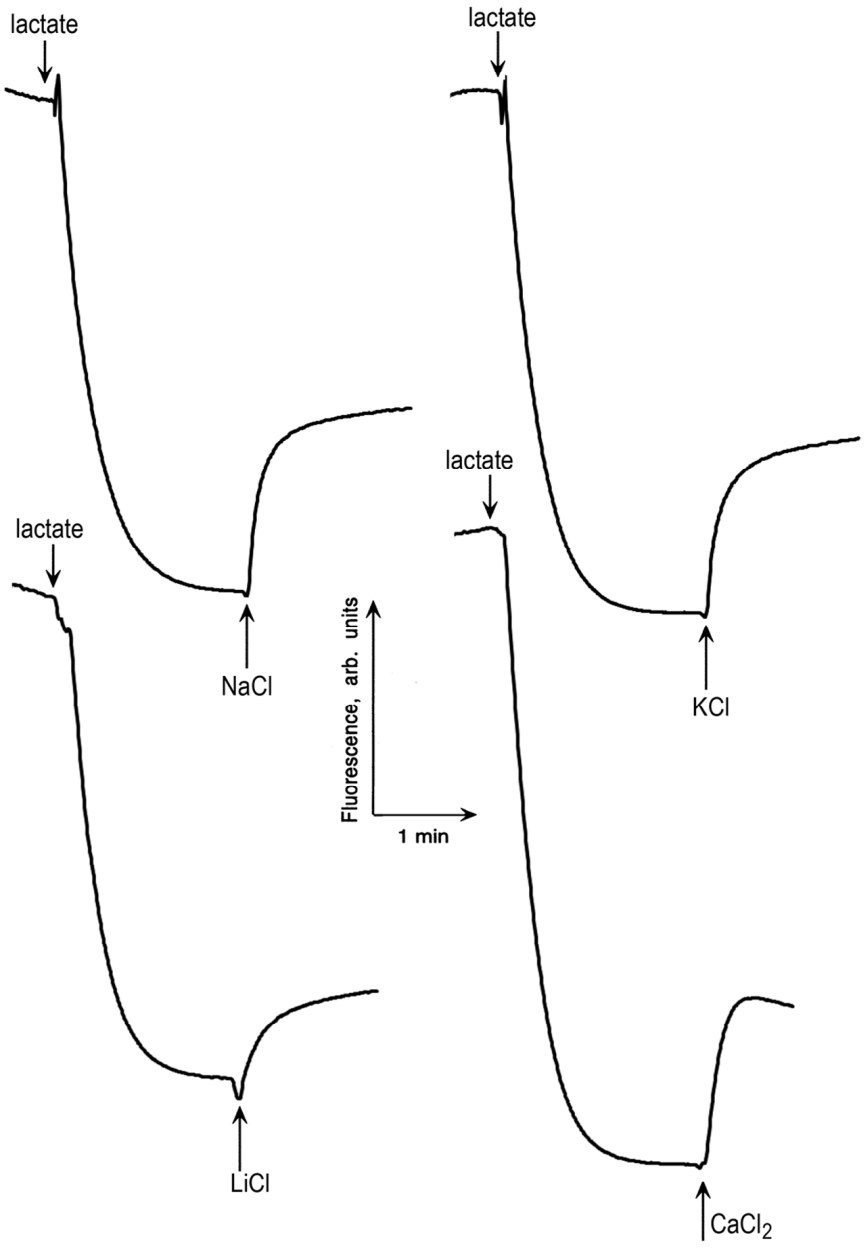


**Fig.3.4.** Yp-NhaP has a broad cation specificity. Assays were performed as described in Materials and Methods at pH 8.0 with 10 mM of a probed cation. Typical traces of at least four independent assays for each probe cation are shown.

### 3.2.2. Concentration dependence of activity for each cation

Figures 3.5 to 3.8 summarize the information about concentration dependence of the activity of Yp-NhaP for its substrate cations. As one can see from the presented data, in the case of $Na^+$ and $K^+$, the activity is smoothly increasing as the concentration of translocated cation increases, thus formally resembling the Michaelis-Menten kinetics (Fig. 3.5 and 3.6). Such behavior is typical for bacterial $Na^+/H^+$ antiporters studied so far (see Padan *et al.*, 2001, 2004; Padan, 2008 and references therein). Interpretation of apparent $K_m$ for these membrane transporters will be briefly discussed below in the section 3.2.3.

However, two other substrates of Yp-NhaP, $Li^+$ and $Ca^{2+}$, do not obey this pattern (Fig. 3.7 and 3.8). In these two cases, inhibition of activity by the excess of substrate is clearly visible. At concentrations of $Li^+$ exceeding 10 mM the activity of Yp-NhaP is progressively decreasing with the growth of $[Li^+]$. The same effect is even more pronounced in the case of $Ca^{2+}$. Here the activity of Yp-NhaP peaks at approximately 2 mM of substrate and sharply declines after that, so that already at 20 mM of $Ca^{2+}$ it is less than 50% of its maximal value. To the best of our knowledge, such inhibition was never observed in bacterial cation-proton antiporters before. It could indicate that Yp-NhaP may be able to bind more than one $Ca^{2+}$ or $Li^+$ ion, and the second act of binding inactivates the antiporter. Clearly, site-directed mutagenesis and kinetic analysis of mutant variants of Yp-NhaP (and, in the future, structural analysis of this antiporter) are required for

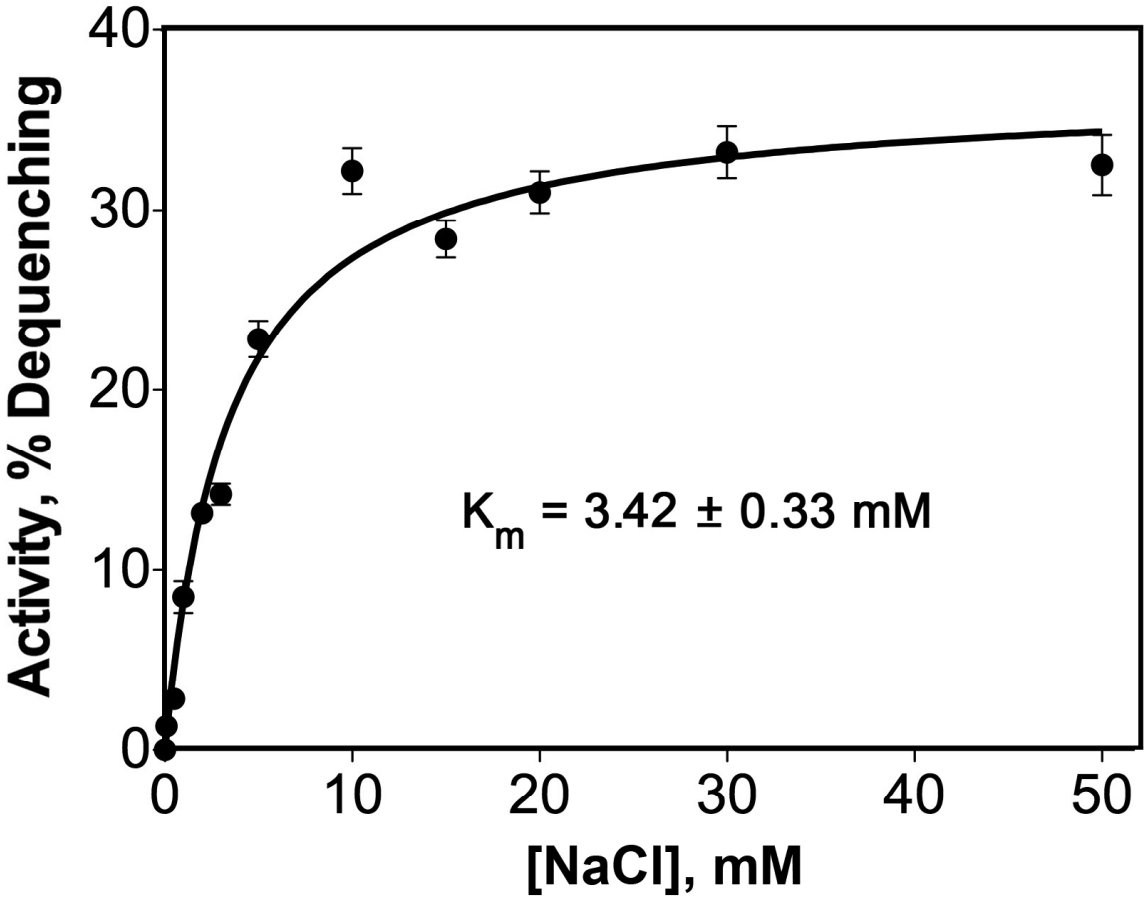


**Fig.3.5.** Concentration dependence of the activity of Yp-NhaP for $Na^+$ ion. Measurements were performed as described in Materials and Methods at pH 8.0.

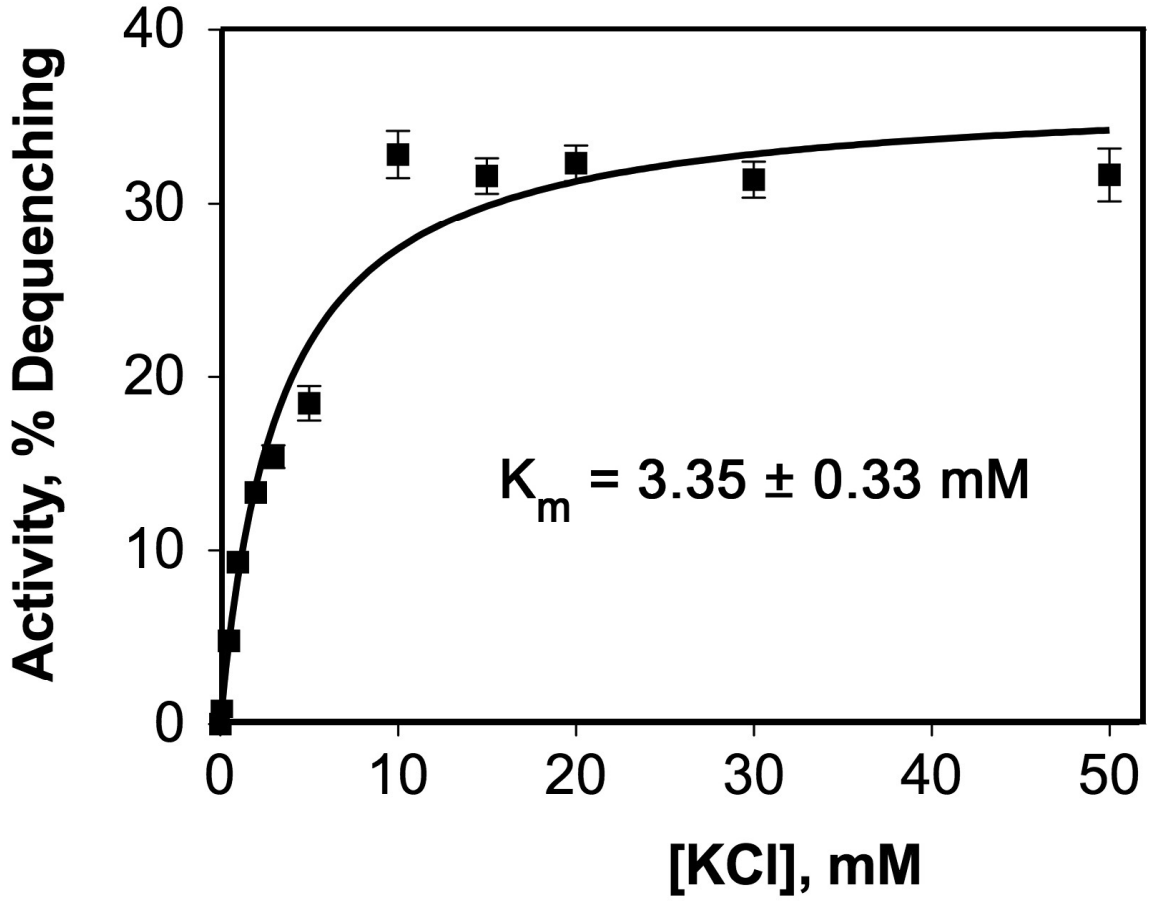


**Fig.3.6.** Concentration dependence of the activity of Yp-NhaP for $K^+$ ion. Measurements were performed as described in Materials and Methods at pH 8.0.

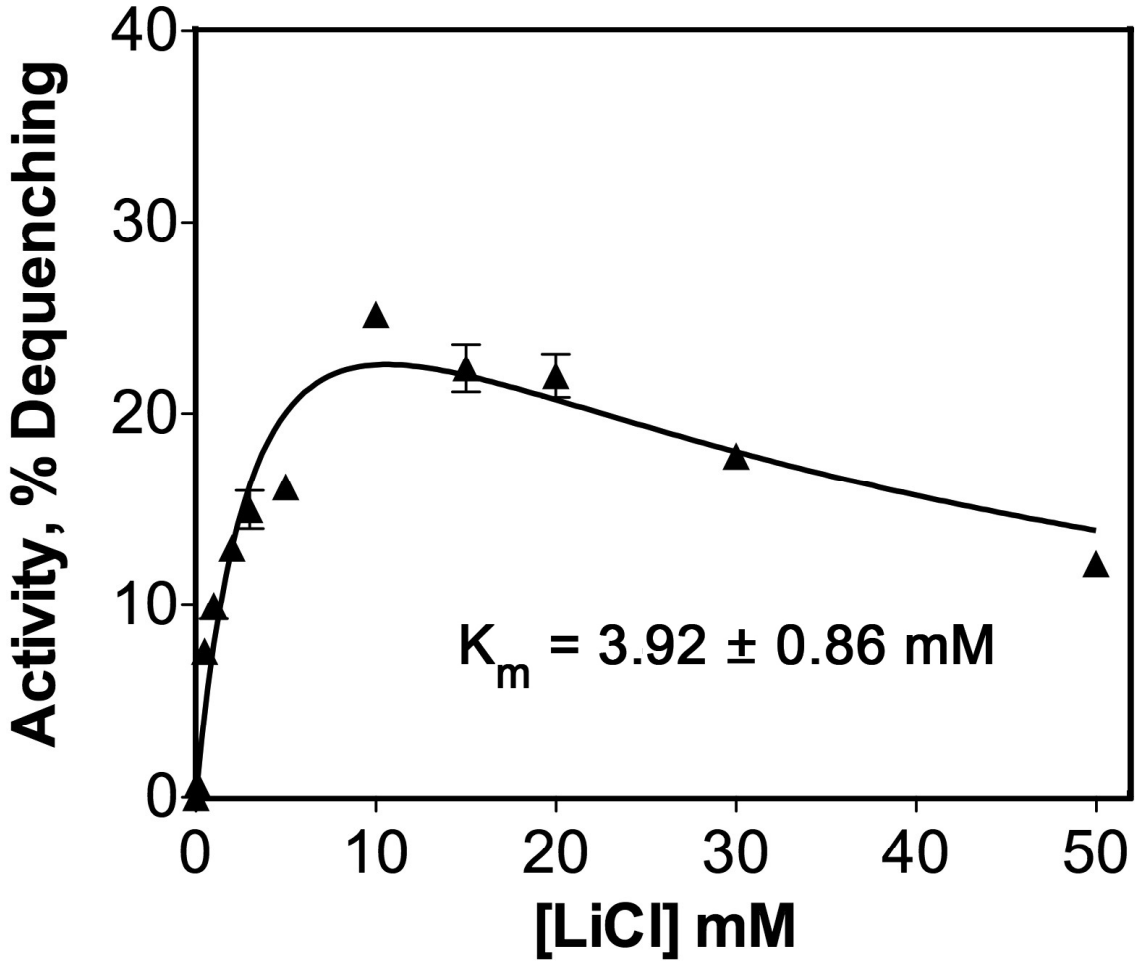


**Fig.3.7.** Concentration dependence of the activity of Yp-NhaP for $Li^+$ ion. Measurements were performed as described in Materials and Methods at pH 8.0.

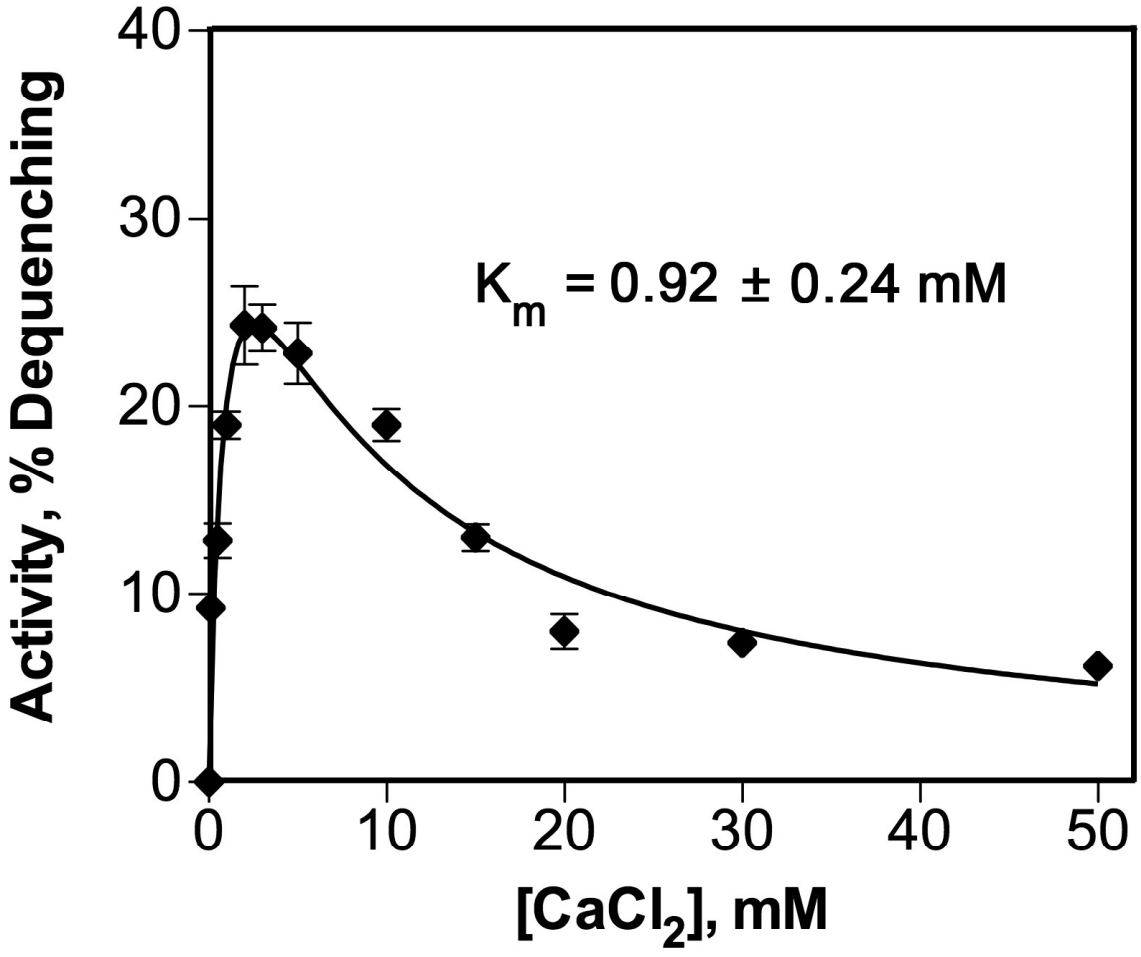


**Fig.3.8.** Concentration dependence of the activity of Yp-NhaP for $Ca^{2+}$ ion. Measurements were performed as described in Materials and Methods at pH 8.0.

the adequate interpretation of this interesting phenomenon. It is also not clear at this moment why $Li^+$, which usually is considered to be a close chemical analog of $Na^+$ as a substrate of the $Na^+/H^+$ exchange in biomembranes (Padan *et al.*, 2001), behaves so differently from $Na^+$ and so similar to $Ca^{2+}$ in the case of Yp-NhaP. There is no clear dependence on the ion radius, because, despite the fact that $Li^+$ and $Ca^{2+}$ are somewhat smaller than $Na^+$ and $K^+$ (0.76 Å and 0.99 Å versus 1.02 Å and 1.38 Å), the difference between $Ca^{2+}$ and $Na^+$ is 0.03 Å only. One could speculate that the hydration status of Yp-NhaP substrates differs from one cation to another. However, it should be mentioned here that for a number of $Na^+$-binding proteins it has been established that they bind $Na^+$ in its dehydrated state, with molecules of water as occasional intermediate ligands (discussed in Mulkidjanian *et al.*, 2008). Perhaps, only the structural analysis of Yp-NhaP co-crystallized with different substrates could give definitive answers to these questions.

### 3.2.3. Apparent $K_m$ values for transported cations

The question about the interpretation of $K_m$ of ion antiport deserves special consideration. As one can see from the general kinetic model of cation-proton antiport shown in Fig.1.2, such a complex process could not be directly approximated by a standard Michaelis-Menten scheme. Nevertheless, term "apparent $K_m$" is widely used in the field as a measure of affinity of a given antiporter toward its substrate(s).

In order to characterize the affinity of Yp-NhaP for its substrate cations, we titrated the dequenching of AO fluorescence in sub-bacterial vesicles isolated from TO114/pYp-NhaP by the concentration of added NaCl, KCl, LiCl and $CaCl_2$ at pH 8.0 (pH optimum of activity for $Ca^{2+}$ and $Li^+$) (Fig. 3.9). The choice of pH 8.0 for the comparison of different substrate cations also seems reasonable because this pH is close to the *in situ* cytoplasmic pH of many pathogenic and non-pathogenic members of human microflora (see, for example, (Padan *et al.*, 2005) and references therein). These measurements yielded the concentration of each cation required for a half-maximal response ($[X^+]_{1/2}$). Although $[X^+]_{1/2}$ is only indirectly related to the actual $K_m$ of the antiporter, this easily measurable parameter is by convention used as a measure of antiporter affinity (see (Resch *et al.*, 2010) for a recent example). With all this in mind, and following the standards accepted in the literature, we shall refer to $[X^+]_{1/2}$ values as $K_m$ of the antiporter for corresponding cation.

The values of $[X^+]_{1/2}$ for $Na^+$, $K^+$ and $Li^+$ turned out to be close to 3.5 mM (see Fig. 3.5-3.7), which are comparable to these found previously for other members of NhaP family (see Table 3). Of note, $K_m$ for $Ca^{2+}$ was somewhat lower, at 0.92 mM (Fig. 3.8). Although the difference between $K_m$ for $Ca^{2+}$ and other cations is not very big, it still indicates that calcium could be a preferable substrate for Yp-NhaP operating *in vivo*. Such expectation is in full agreement with our working hypothesis about Yp-NhaP as an integral part of $Ca^{2+}$ homeostasis in *Y. pestis*.

### 3.3. The pH-profiles of activity of Yp-NhaP

Very interesting results were obtained in screening of pH-dependence of the activity of Yp-NhaP with different substrates. When assayed in inside-out vesicles of TO114/pYp-NhaP by the addition of 10 mM of probe cations, Yp-NhaP demonstrated two types of pH-profiles of activity depending on the translocated cation:

(1) The bell-shaped pH profile of $Li^+/H^+$ as well as $Ca^{2+}/H^+$ antiport activity with a maximum at pH close to 8.0 (Fig. 3.9, triangles and diamonds). Practically no activity with either cation was detected at pH 6.5 and below.

(2) In the case of $Na^+$ and $K^+$, the antiporter showed gradual increase of activity starting from pH = 6.5 up to pH of 9.0, reaching approximately 40% of the AO fluorescence dequenching, without any measurable difference between these two alkali cations (Fig. 3.9, circles and squares).

Curiously, with $Li^+$ and $Ca^{2+}$ the antiporter once again demonstrated very similar behavior, which was very different from that with $Na^+$ and $K^+$ (compare Fig. 3.9 and Fig. 3.5-3.8). Therefore, all substrates of Yp-NhaP fall into two types: (i) those whose excess inhibits the antiporter; they also have the bell-shaped pH-profile of activity peaking at pH ~8.0. $Li^+$ and $Ca^{2+}$ belong to this type; (ii) excess of $Na^+$ or $K^+$, on the other hand, does not inhibit the $Na^+/H^+$ and $K^+/H^+$ antiport, respectively. Activity with these cations smoothly increases from pH 6.5 to 9.0.

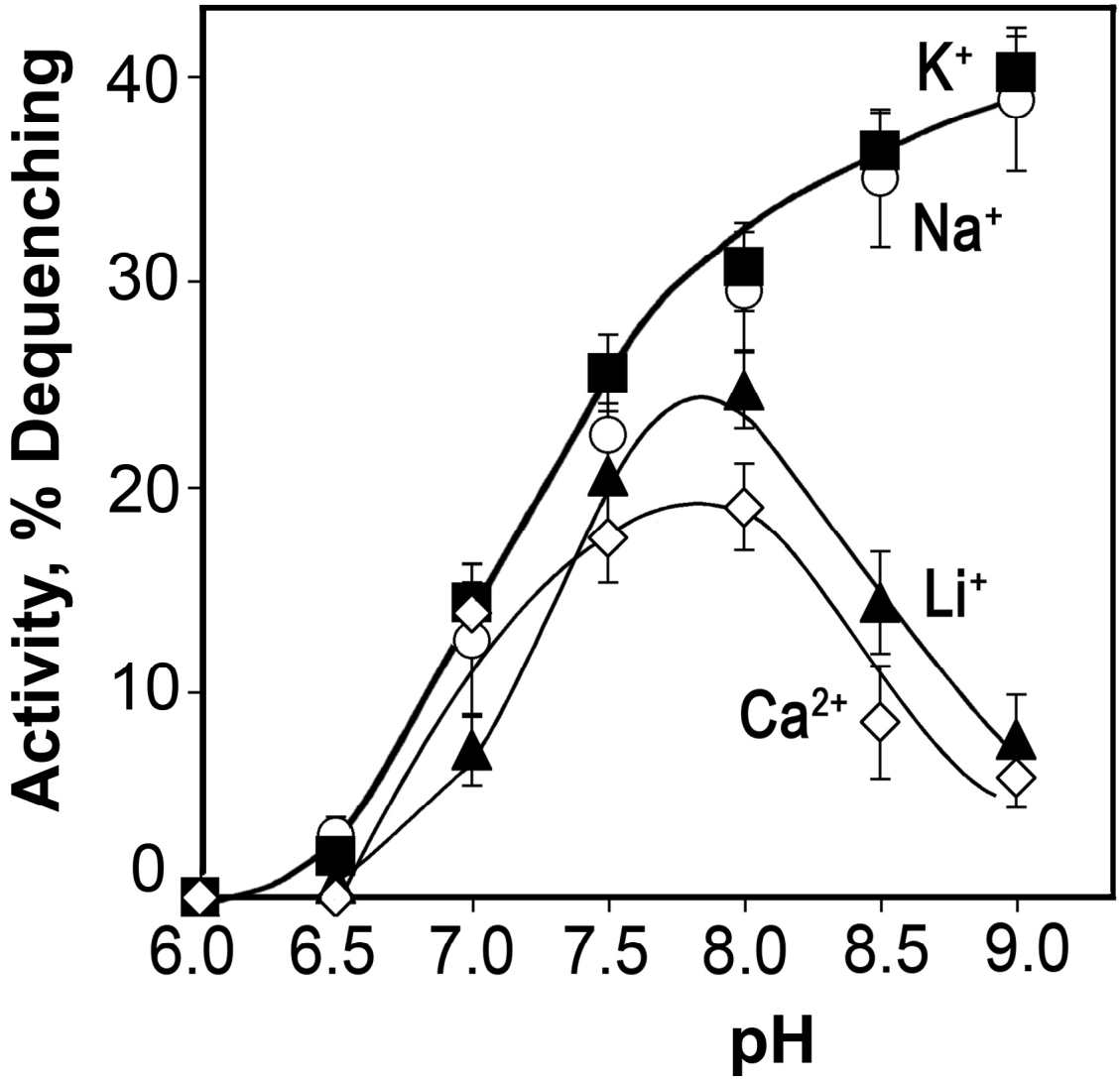


**Fig.3.9.** The pH profiles of the activity of Yp-NhaP for each substrate cation. Measurements were performed as described in Materials and Methods.

### 3.4. Ion competition assays

As it is discussed in the above sections, Yp-NhaP shows very similar affinities for all its substrate cations, which is reflected in the close values of apparent $K_m$ (Fig. 3.5-3.8). Therefore, in order to establish what cation(s) are preferably transported by Yp-NhaP *in vivo*, it was important to compare reciprocal effects of substrate cations on the cation/proton antiport activity of Yp-NhaP. Figures 3.10-3.15 summarize the data about the interplay between $K^+$, $Na^+$ and $Ca^{2+}$. Lithium was not included in these assays because its concentration in the environment of *Y. pesis* at any stage of its life cycle is negligible and thus $Li^+$ could not be a physiological substrate for the antiporter. We are leaving this aspect for future studies.

In this series of experiments, varying concentrations of one cation ($X^+$) were added into the experimental buffer (pH 8.0) prior lactate. After a respiratory-driven $\Delta$pH was established in the presence of a given [$X^+$], 10 mM of second cation ($Y^+$) were added to initiate $Y^+/H^+$ antiport. If $Y^+$ competes with $X^+$ for the antiporter, increasing concentrations of $X^+$ should progressively inhibit $Y^+/H^+$ antiport (and *vice versa*). Since the membrane vesicles used in these experiments are of inside-out orientation, the salt composition and pH of the external buffer imitated that of the bacterial cytoplasm.

It turned out that already 0.1 mM of $Na^+$ added to the experimental medium (which is below an average sodium concentrations in the bacterial cytoplasm) significantly inhibited the Vc-NhaP2-mediated $K^+/H^+$ antiport, leaving slightly more

than half of its initial activity (Fig. 3.10). 5 mM of $Na^+$ (close to average intra-bacterial levels of $Na^+$) abolished the process completely. Such a strong inhibition makes it unlikely that Yp-NhaP mediates considerable $K^+/H^+$ antiport *in vivo*. While the $Na^+/H^+$ antiport remained measurable in the presence of 10 mM of added $K^+$, it became non-detectable at $[K^+]$ = 100 mM, a concentration that is typical for cytoplasmic $K^+$ in enterobacterial species (Fig. 3.11). Taken together these data apparently exclude the possibility of Yp-NhaP-mediated $Na^+/H^+$ as well as $K^+/H^+$ exchange under physiological conditions, leaving $Ca^{2+}/H^+$ antiport as the most probable mode of Yp-NhaP activity *in vivo*.

Indeed, neither externally added $Na^+$ (Fig. 3.12) nor $K^+$ (Fig. 3.13) inhibited the $Ca^{2+}/H^+$ antiport through Yp-NhaP, even at 0.2 M, concentration exceeding the physiological levels for both alkali cations. Of note, the addition of as much as 10 mM of $Ca^{2+}$ inhibited both $Na^+/H^+$ and $K^+/H^+$ antiport only partially (Fig. 3.14-3.15). This leaves an interesting possibility of the $Ca^{2+}/Na^+$ exchange through Yp-NhaP. From physiological point of view, such heterologous ion exchange could be beneficial for cells of *Y. pestis* immersed into a sodium-rich medium (such as blood). They could use $\Delta$pNa on the membrane (created and maintained by NQR and NhaA) to prevent intracellular accumulation of $Ca^{2+}$.

Another important parameter determining what activity is Yp-NhaP mediating *in vivo*, is stoichiometry of ion exchange: while an electroneutral antiporter can be energized by $\Delta$pH only, electrogenic one can use both $\Delta$pH and $\Delta\psi$ to expel substrate cations from the cytoplasm.

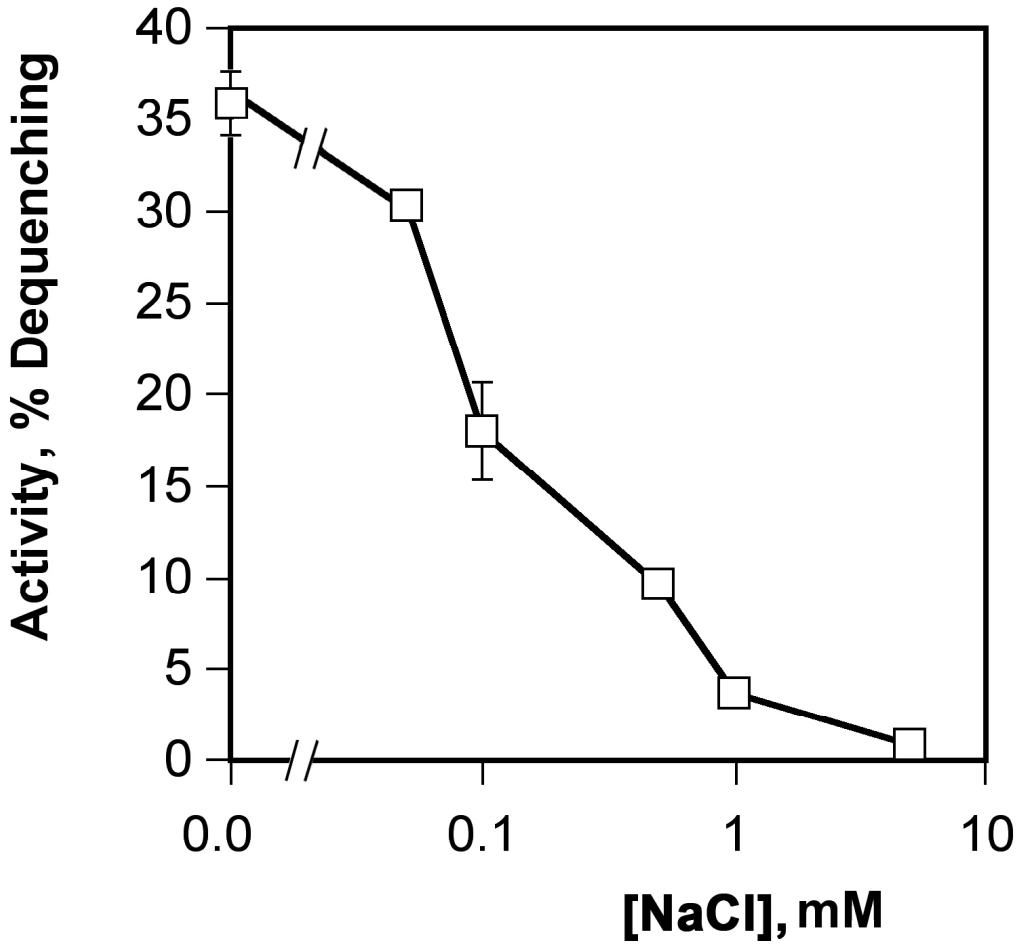


**Fig.3.10.** Externally added $Na^+$ inhibits $K^+/H^+$ antiport mediated by Yp-NhaP.

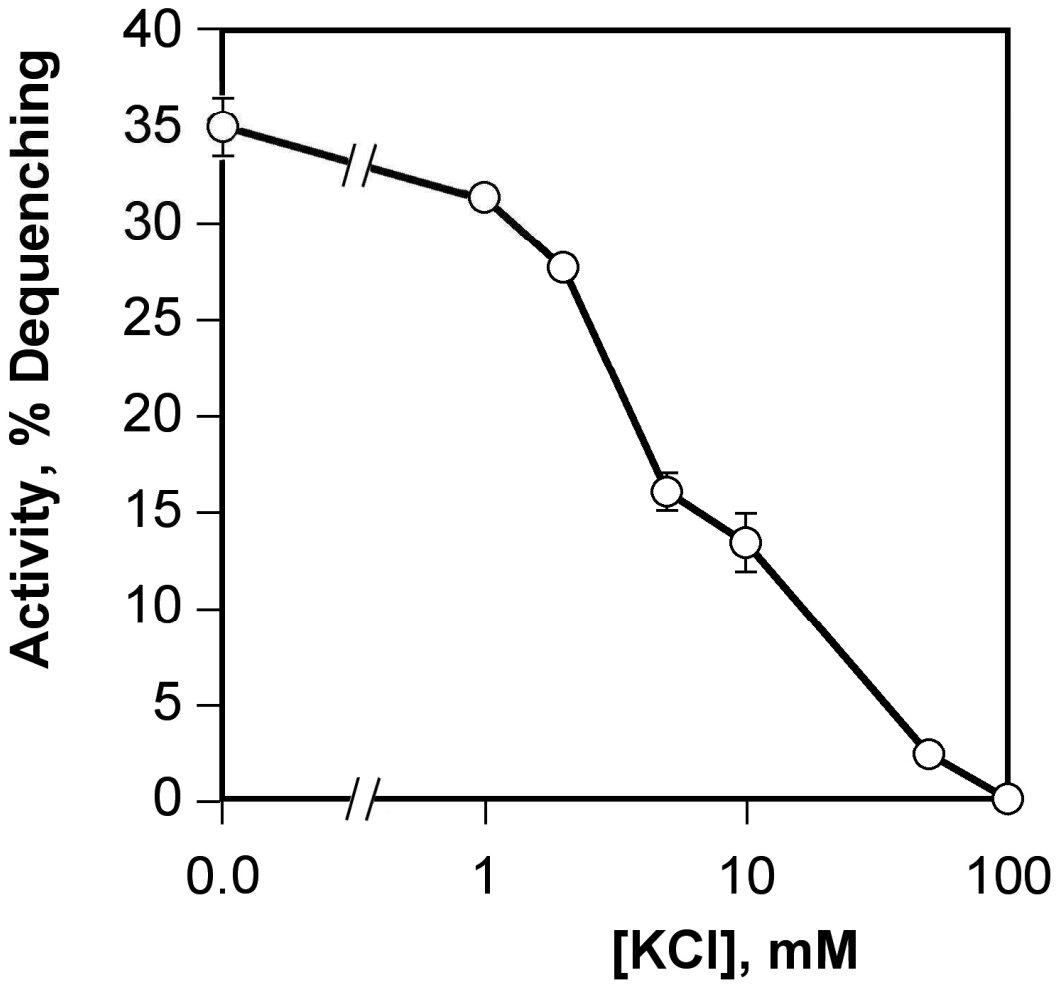


**Fig.3.11.** Externally added $K^+$ inhibits $Na^+/H^+$ antiport mediated by Yp-NhaP.

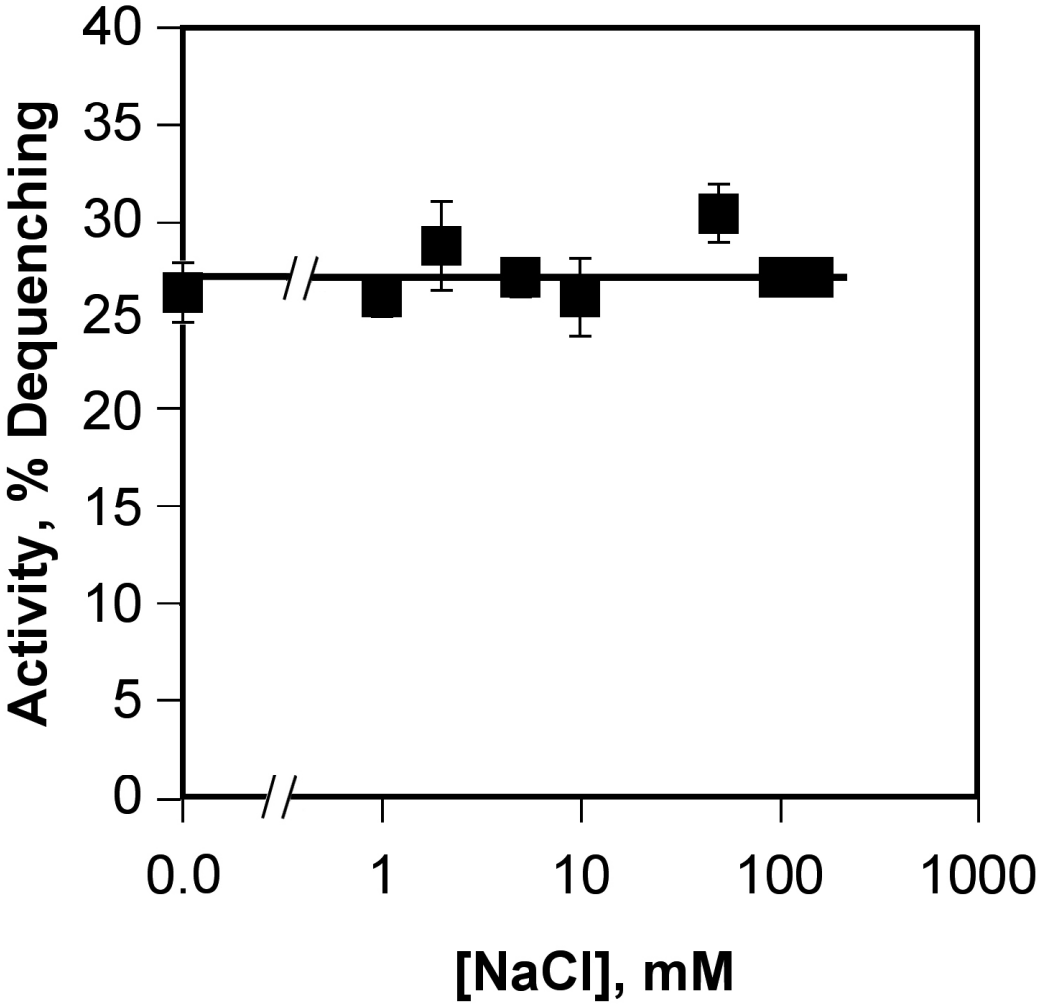


**Fig.3.12.** Externally added $Na^+$ does not inhibit $Ca^{2+}/H^+$ antiport mediated by Yp-NhaP.

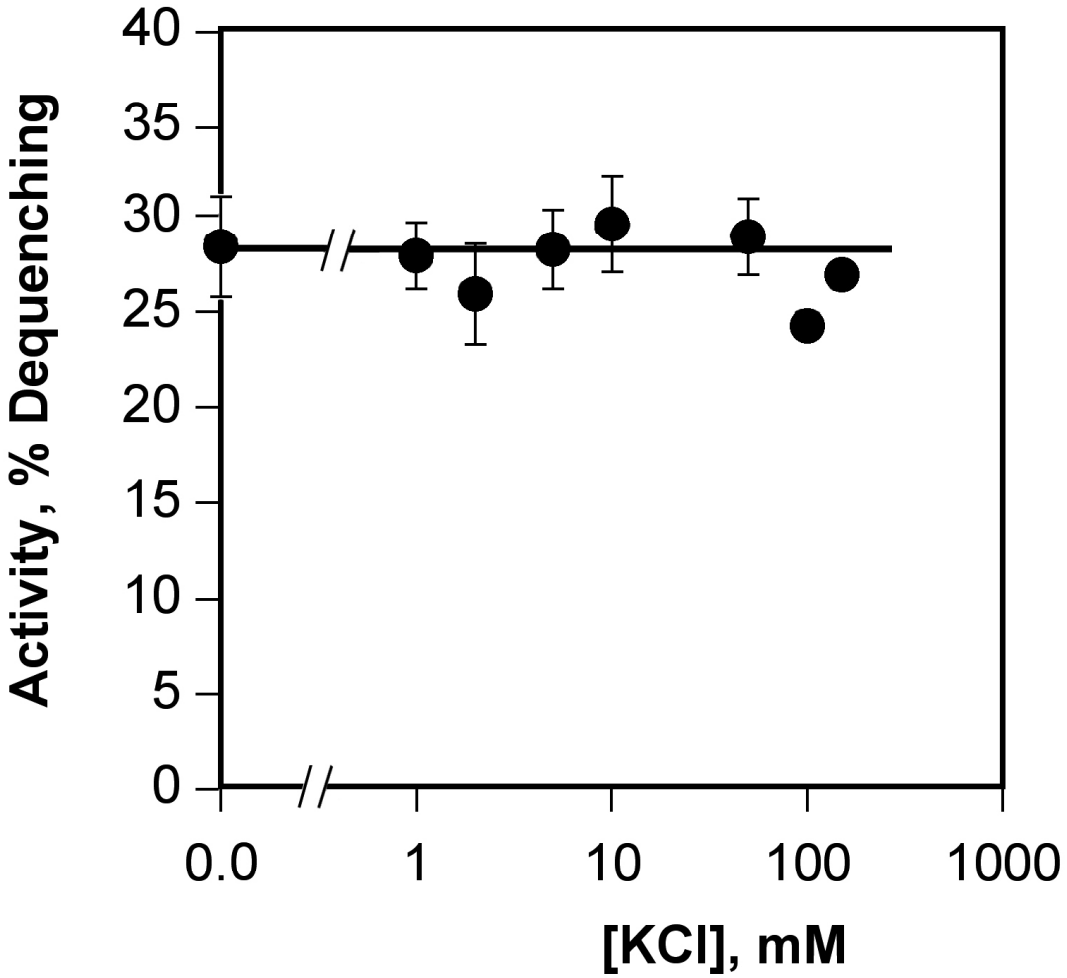


**Fig.3.13.** Externally added $K^+$ does not inhibit $Ca^{2+}/H^+$ antiport mediated by Yp-NhaP.

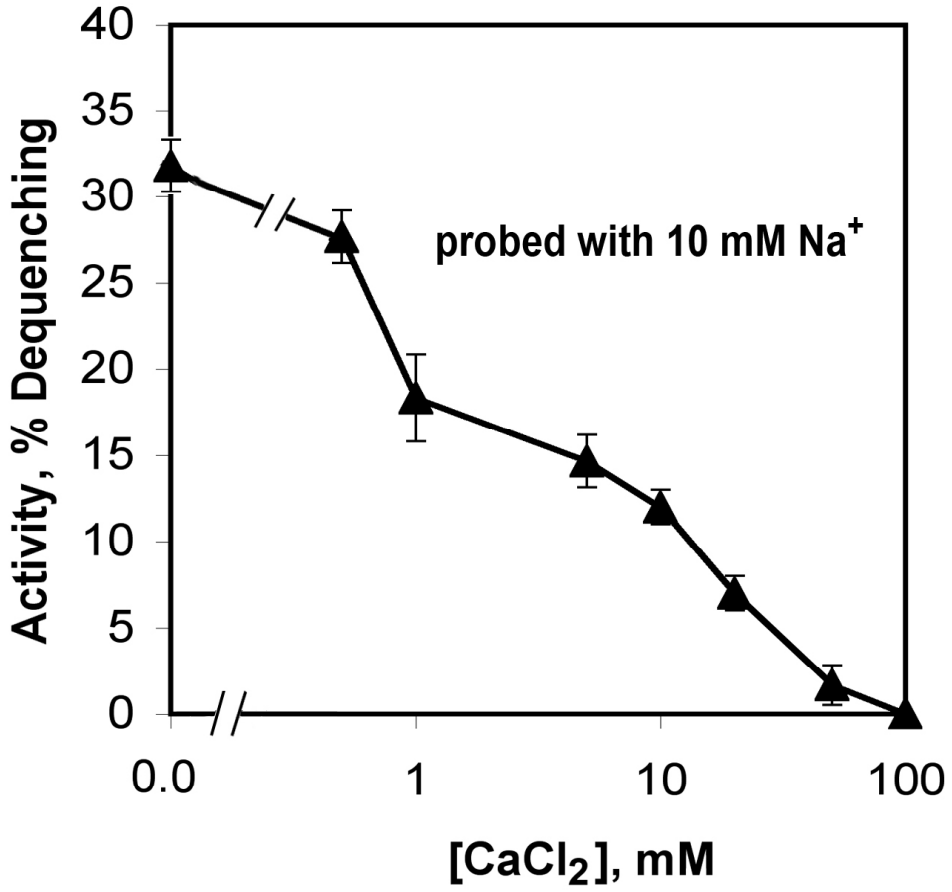


**Fig.3.14.** Externally added $Ca^{2+}$ inhibits $Na^+/H^+$ antiport mediated by Yp-NhaP. See the text for details.

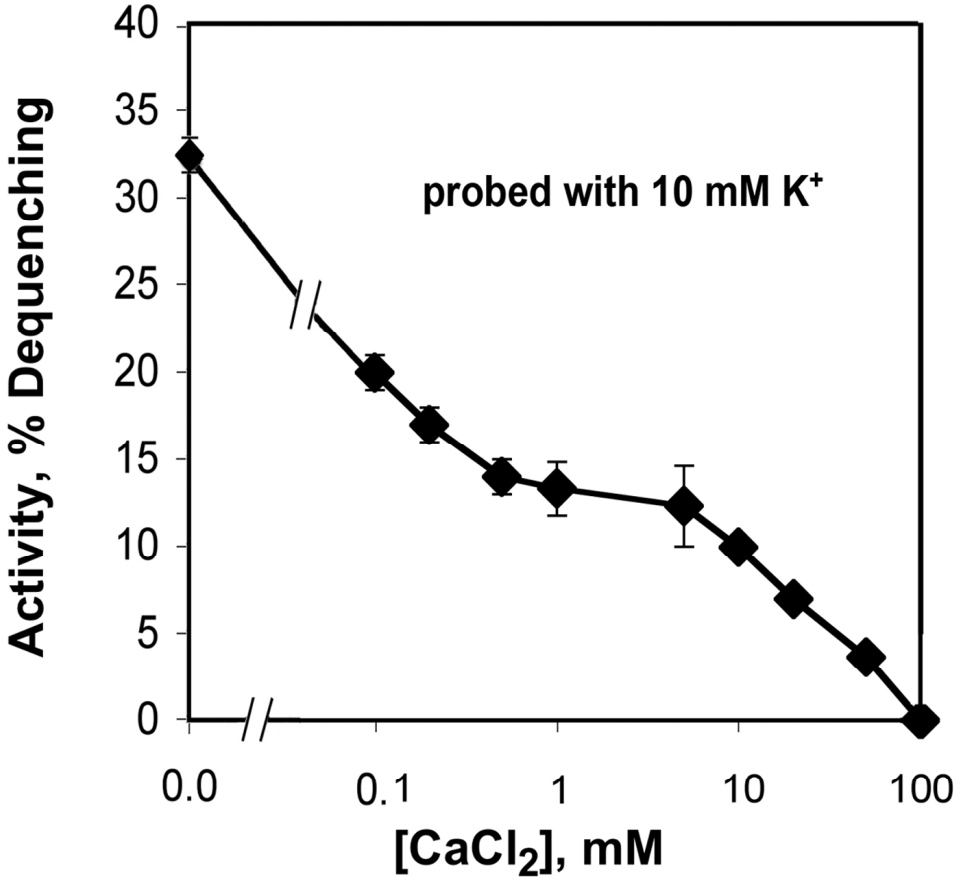


**Fig.3.15.** Externally added $Ca^{2+}$ inhibits $K^+/H^+$ antiport mediated by Yp-NhaP. See the text for details.

### 3.5. Probing the stoichiometry of antiport

The stoichiometry of proton-cation antiport (i.e., the number of protons exchanged per each substrate cation) is one of fundamental functional characteristics of any antiporter. However, the kinetic data discussed in the above sections do not determine the stoichiometry of the Yp-NhaP-mediated antiport by themselves.

To probe the stoichiometry of Vc-NhaP2, inside-out membrane vesicles isolated from TO114/pYp-NhaP transformants were assayed for $\Delta\psi$ in chloride-free, cation-free (sorbitol-based) experimental buffer with the $\Delta\psi$-sensitive dye, Oxonol V. While such approach cannot give an exact value of the proton-cation antiport stoichiometry, it can easily distinguish between electroneutral and electrogenic antiport (see, for example, Resch *et al.*, 2010). If the process is electroneutral, level of $\Delta\psi$ on the membrane of energized vesicles should be insensitive to the addition of a substrate cation. But if the antiport is electrogenic, the net charge movement across the membrane resulting from the antiport must cause (at least) partial depolarization and establishment of a new, lower steady-state level of $\Delta\psi$.

In our experiments, 20mM diethanolamine was added to the vesicle suspension 5 minutes prior to addition of Oxonol V, in order to maximize the respiration-generated $\Delta\psi$. Energization by lactate led to the rapid generation of the respiratory $\Delta\psi$ in TO114/pYp-NhaP vesicles (Fig. 3.16). However, the

addition of 5 mM of any alkali cation ($K^+$, $Li^+$, or $Na^+$ (Fig. 3.16, two upper and lower left traces) did not result in depolarization, thus indicating the electroneutral nature of the cation/$H^+$ exchange mediated by Vc-NhaP2 i.e., exchanging one alkali cation per one proton. The control addition of protonophore CCCP (which short-circuits the membrane for the proton current and, in the presence of penetrating diethanolamine, must cause immediate collapse of $\Delta\psi$) completely dissipated respiratory $\Delta\psi$ in all cases (the last addition in each trace of Fig. 3.16). This control shows that the changes of fluorescence of Oxonol V observed in our experiments are indeed reflecting the transmembrane electric potential difference.

Unexpectedly enough, the same result was obtained for the Yp-NhaP-mediated $Ca^{2+}/H^+$ antiport (Fig. 3.16, lower right trace). Therefore, it turned out that Yp-NhaP catalyzes the electroneutral ion exchange of $H^+$ for monovalent alkali cations as well as divalent $Ca^{2+}$! One conceivable explanation for this observation is that Yp-NhaP has a variable stiochiometry for protons: it exchanges $1H^+$ per each alkali cation ($Na^+$, $K^+$ or $Li^+$) but $2H^+$ per each $Ca^{2+}$ ion in each catalytic cycle. As far as we know, this would be the first such case among bacterial antiporters exchanging inorganic cations.

But this explanation raises a question: how the protonation state of Yp-NhaP might be regulated by substrate cations (or vice versa)? The standard kinetic model of cation-proton exchange implies that the reversible protonation of antiporter and cation binding-release are separated and mutually independent (see Fig. 1.2). It is hard to see how this might be not true in the case of Yp-NhaP.

Alternatively, one could suggest that cation-binding site of Yp-NhaP is large enough for the antiporter to exchange either 1 $Ca^{2+}$ ion for $2H^+$ or *two alkali cations for* $2H^+$ in each catalytic cycle. In other words, it would mean that the *minimal* stoichiometry of electroneutral exchange ($1X^+/1H^+$) for monovalent cations is different from the *actual* one, which is ($2X^+/2H^+$). But if so, would "mixed" $1Na^+1K^+/2H^+$ exchange also possible in Yp-NhaP?

Apparently, there are also other interesting possibilities that would lead to a significant revision of the universally accepted model illustrated by Fig. 1.2, such as an ordered binding of the substrate cations and proton(s) at the same side of the membrane. It seems, however, that to obtain a convincing evidence for one such scheme or another, Yp-NhaP must be purified and incorporated into proteoliposomes, where all modes of its activity cold be studied without interference from other ion transporters and with high precision.

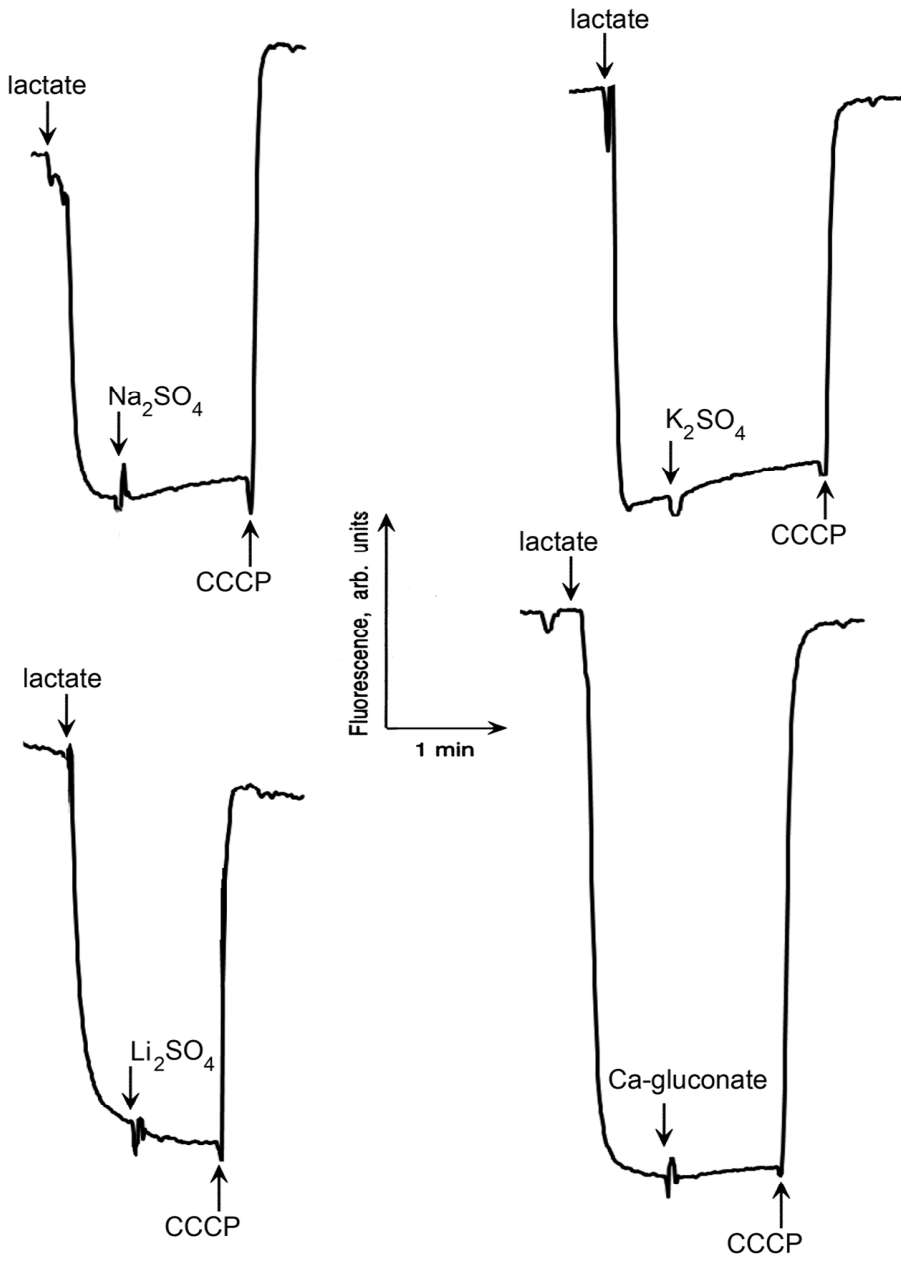


**Fig.3.16.** Cation/$H^+$ antiport mediated by Yp-NhaP does nor perturb $\Delta\psi$ on the membrane.

### 3.6. Growth properties of Yp-NhaP deletion mutant

The data on the ion competition in Yp-NhaP obtained in the experimental model of TO114/pYp-NhaP vesicles (Fig. 3.10-3.11) suggest that under realistic *in vivo* conditions (cytoplasmic [$K^+$] at 100 mM or higher, [$Na^+$] between 5 and 15 mM, and submillimolar [$Ca^{2+}$]) this antiporter can hardly mediate either $Na^+/H^+$ or $K^+/H^+$ exchange due to the mutual inhibition by alkali cations. On the other hand, even huge excess of $Na^+$ or $K^+$ had no effect on $Ca^{2+}/H^+$ antiport mediated by Yp-NhaP in membrane vesicles (Fig. 3.12-3.13). Of note, 50% of inhibition of either $Na^+/H^+$ or $K^+/H^+$ exchange required about 5 mM of added [$Ca^{2+}$] (Fig. 3.14-3.15). Based on these results, one could expect that *in vivo* the $Ca^{2+}/H^+$ antiport is the only mode of activity associated with Yp-NhaP.

Therefore, from the physiological point of view, elimination of functional Yp-NhaP in the chromosomal deletion mutant of *Y. pestis* should not affect its resistance to alkali cations. To check this prediction experimentally, parental strain of *Y. pests* KIM5 (YpWT), as well as its isogenic *Yp-nhaP* deletion mutant (YpΔNhaP, kindly provided by Dr. C. Häse, Oregon State University) and the same mutant expressing Yp-NhaP *in trans* (YpΔNhaP/pYp-NhaP) were grown in batch cultures aerobically at ambient temperature overnight as described in Materials and Methods in the presence of varying concentrations of specified alkali cations (Fig. 3.17-3.19). Growth experiments were performed at pH 6.0, 7.2 and 8.0. Both YpWT and YpΔNhaP were transformed with “empty” pBAD24 plasmid to make growth conditions standardized for all three strains used. Three

to four parallels were set up for each strain under any given growth conditions. Bacterial growth was monitored as turbidity of culture at 600 nm, and growth yields were plotted as functions of concentration of added alkali cation. As one can see from the data presented in Fig. 3.17 and Fig. 3.19, all three *Y. pestis* strains showed quite significant resistance to environmental $Na^+$ and $K^+$ at all three pH tested, showing stable growth up to 0.5 M of added salt. Resistance to $Li^+$ ions was somewhat lower, especially at higher pH (Fig. 3.18), which is not surprising, because $Li^+$ is known to be much more toxic than either $Na^+$ or $K^+$ (Padan *et al.*, 2001).

Most importantly, the deletion of Yp-NhaP gene did not at all affect the resistance of the YpΔNhaP cells to alkali cations. Therefore, in full accord with our data obtained in sub-bacterial vesicles, Yp-NhaP does not contribute to the homeostasis of either $Na^+$ or $K^+$ in *Y. pestis*. High halotolerance in this bacterium is obviously maintained at sufficient level by concerted operation of NQR and NhaA (see Introduction and Literature Review, Table 1 in particular). As to the resistance to potassium, apparently there are primary and/or secondary $K^+$ pumps in the membrane of *Y. pestis* different from Yp-NhaP that are responsible for it. Detailed analysis of potassium circulation in *Y. pestis* is beyond the scope of the present work, but it should be mentioned here that a number of putative potassium exporting systems is annotated in the *Y. pestis* KIM genome database (at http://cmr.jcvi.org), including RosB (putative $K^+$ efflux protein), Kdp system ($K^+$-motive ATPase) and KefB ($K^+$ efflux NEM-activable $K^+/H^+$ antiporter).

Unexpected to some extent was the finding that the resistance of YpΔNhaP cells to external $Ca^{2+}$ remained unaffected, as well (Fig. 3.20). Lowered growth yield in this particular series of experiments is due to the fact that the synthetic growth medium was used here to avoid massive precipitation of added $Ca^{2+}$ by the components of rich growth media usually used to propagate *Y. pestis* (compare media formulations in Materials and Methods). One would suggest that, if Yp-NhaP indeed operates as a $Ca^{2+}/H^{+}$ antiporter under physiological conditions, its elimination should be reflected in the phenotype of the deletion mutant. Nevertheless, at any pH checked, there was absolutely no difference in the growth yield between YpWT and YpΔNhaP strain (Fig. 3.20). Apparently, the remaining components of the $Ca^{2+}$ circulation machinery, namely ChaA antiporter, $Ca^{2+}$-motive ATPase and putative $Ca^{2+}/H^{+}$ antiporter YrbG (see Table 2) were able to compensate for the loss of functional Yp-NhaP.

Thus, at the present moment physiological role of Yp-NhaP remains obscure. One must take into account, however, that our search for a possible mutant phenotype was based on growth yield assays of aerobic batch cultures incubated at ambient temperature only. We did not explore systematically the growth of our *Y. pestis* strains at 37ºC, because this higher temperature markedly inhibits growth yield (Dr. Winogrodzky, unpublished observations). Since nothing is known yet about the regulation of expression of Yp-NhaP, it is possible that phenotype of YpΔNhaP will be evident only in animal model of *Y. pestis* infection, given the tightly closed life cycle of this pathogen.

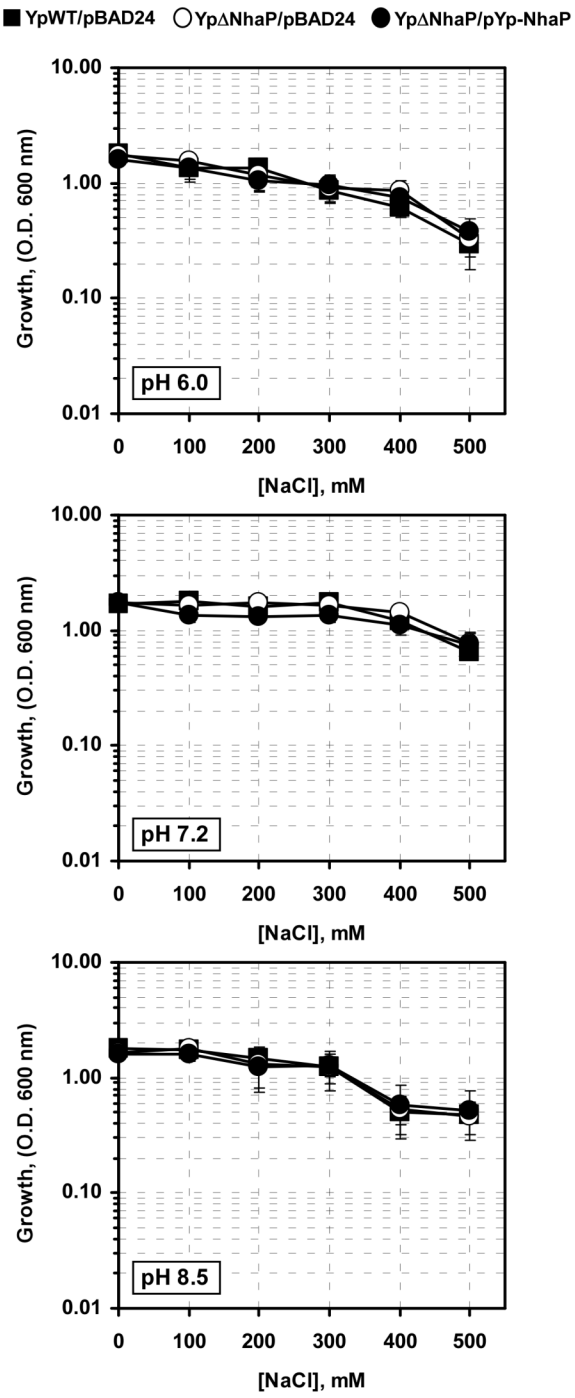


**Fig.3.17.** Chromosomal deletion of *Yp-nhaP* gene does not affect the resistance of *Y. pestis* to external $Na^+$ ions. See the text for discussion.

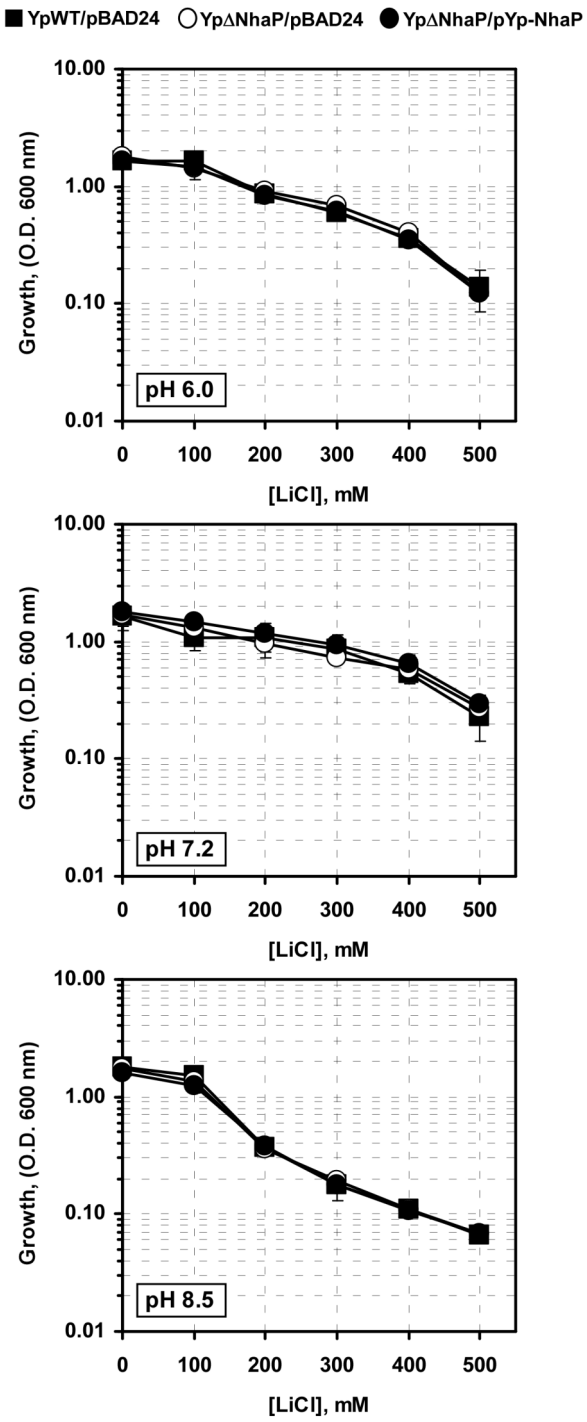


**Fig.3.18.** Chromosomal deletion of *Yp-nhaP* gene does not affect the resistance of *Y. pestis* to external $Li^+$ ions. See the text for discussion.

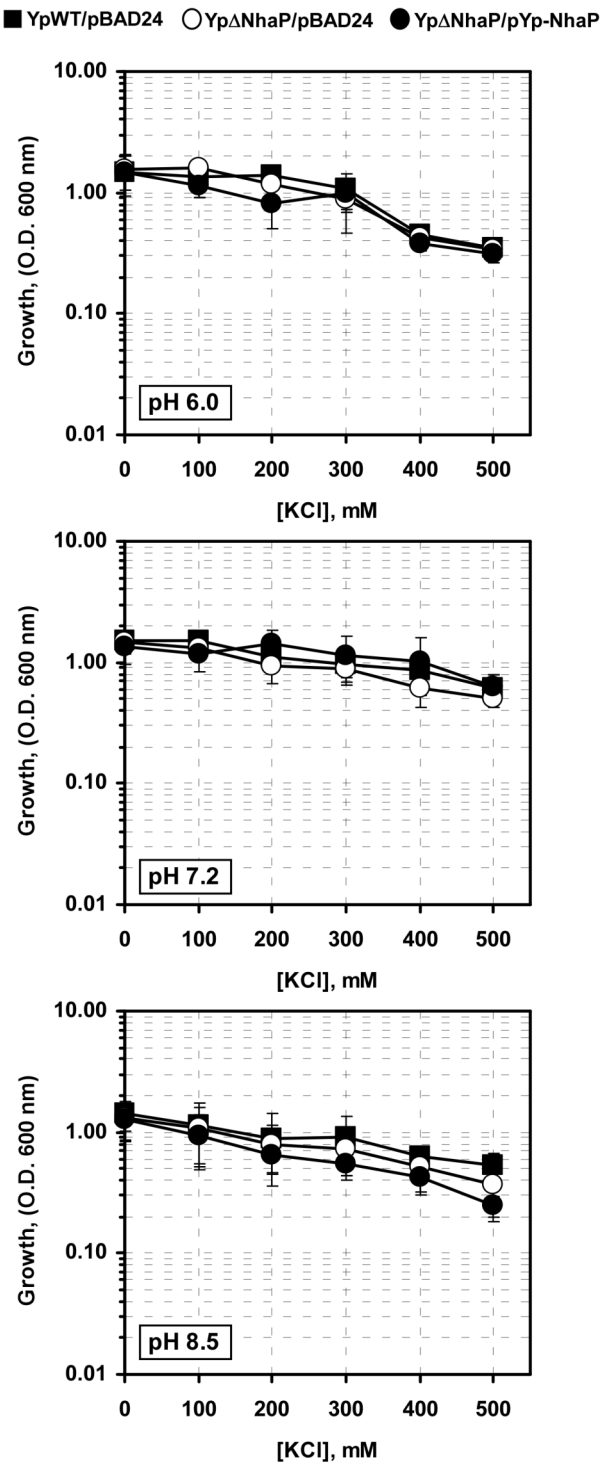


**Fig.3.19.** Chromosomal deletion of *Yp-nhaP* gene does not affect the resistance of *Y. pestis* to external $K^+$ ions. See the text for discussion.

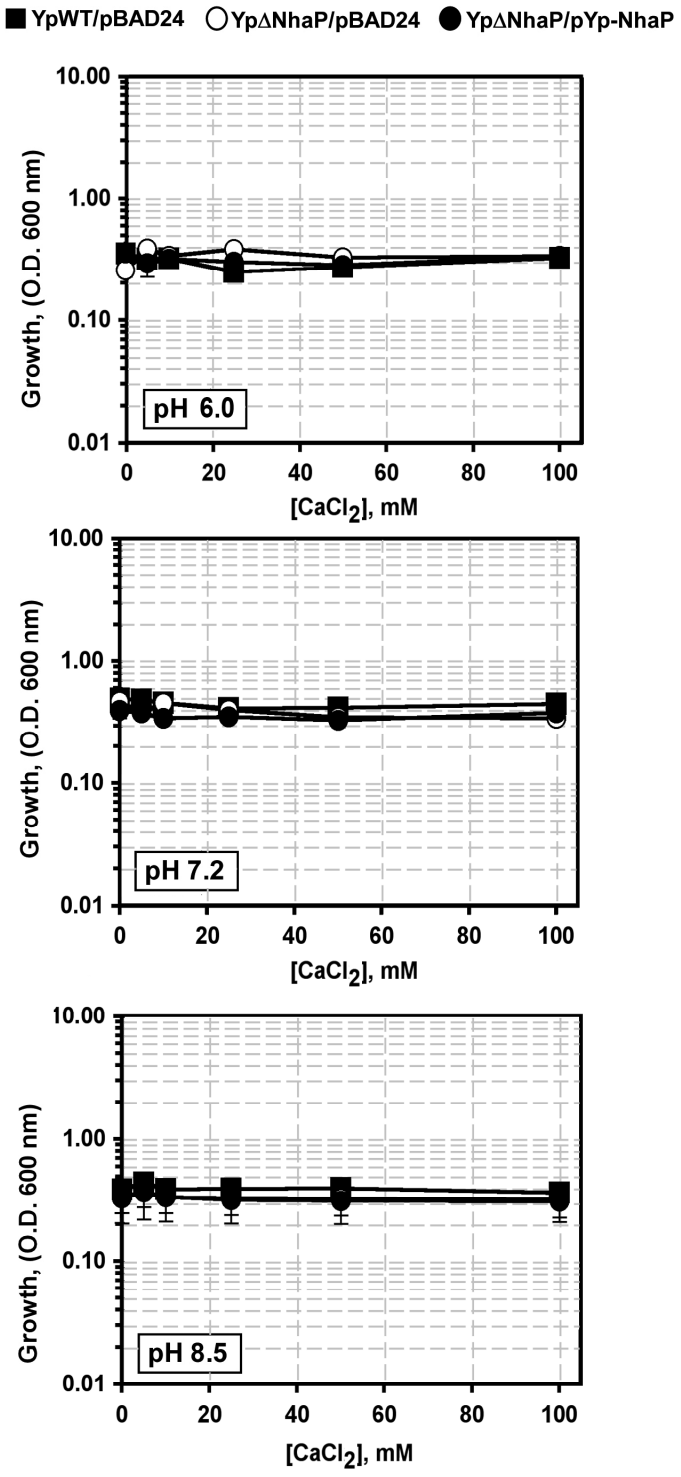


**Fig.3.20.** Chromosomal deletion of *Yp-nhaP* gene does not affect the resistance of *Y. pestis* to external $Ca^{2+}$ ions. See the text for discussion.

## 4. CONCLUSIONS

**1]** Successful cloning of Yp-NhaP and its functional expression in *E. coli* confirms that the putative *Yp-nhaP* gene at the locus YPO3630 indeed encodes a chemiosmotically active cation-proton antiporter of the NhaP type, in the accordance with the automated annotation published in the Web. A conclusion of this kind is not trivial in the case of *Y. pestis*, whose genome contains a very high percentage of pseudo-genes.

**2]** Yp-NhaP has a broad substrate specificity, catalyzing the exchange of protons with alkali cations $Na^+$, $K^+$ and $Li^+$, as well as with divalent $Ca^{2+}$. The experimental observation of Yp-NhaP mediating $Ca^{2+}/H^+$ antiport supports our initial hypothesis that a positively charged arginine in position 83 (in the Yp-NhaP enumeration) might be a structural predictor of the ability of an antiporter of NhaP type to use calcium ion as a substrate.

**3]** Assays of activity in inside-out sub-bacterial vesicles revealed that the substrates of Yp-NhaP fall into the two distinct types: (i) in the case of $Li^+$ and $Ca^{2+}$, the excess of substrate inhibits the antiport of this cation with proton; $Li^+$ and $Ca^{2+}$ also have the identical bell-shaped pH-profile of activity peaking at pH ~8.0; (ii) excess of $Na^+$ or $K^+$ does not inhibit the $Na^+/H^+$ and $K^+/H^+$ antiport, respectively. Activity of Yp-NhaP with these cations smoothly increases over the pH range from 6.5 to 9.0 without a clear peak or plateau.

**4]** The values of apparent $K_m$ for the proton-cation antiport with $Na^+$, $K^+$ and $Li^+$ were found to be close to 3.5 mM, while $K_m$ for $Ca^{2+}$ was somewhat lower, at 0.92 mM. This indicates that calcium could be a preferable substrate for Yp-NhaP operating *in vivo*, as predicted in our working hypothesis about Yp-NhaP as an integral part of $Ca^{2+}$ homeostasis in *Y. pestis*.

**5]** The idea about $Ca^{2+}$ as a preferable substrate for Yp-NhaP was further supported in the experiments concerning the cation competition. Indeed, even huge excess of $Na^+$ or $K^+$ had no effect on $Ca^{2+}/H^+$ antiport assayed in membrane vesicles. In contrast, $Na^+$ and $K^+$ were found to be mutual inhibitors, thus indicating that, unlike $Ca^{2+}$, they possibly compete for an identical set of coordination ligands within the active site of Yp-NhaP. Since $Li^+$ is not a physiological substrate of any antiporter, we are leaving the characterization of this substrate of Yp-NhaP for future studies.

**6]** The Yp-NhaP-mediated cation-proton antiport with any substrate did not disturb $\Delta\psi$ on the membrane of vesicles, indicating that the process was electroneutral in all cases. This could be explained by a variable stoichiometry of the exchange for proton: $1H^+$ per each alkali cation ($Na^+$, $K^+$ or $Li^+$) but $2H^+$ per each $Ca^{2+}$ ion. Alternatively, Yp-NhaP may exchange 2 alkali cations per $2H^+$ in each catalytic cycle.

**7]** Deletion of the chromosomal *Yp-nhaP* gene did not affect the resistance of *Y. pestis* KIM5 strain to the external $Na^+$, $K^+$, $Li^+$ or $Ca^{2+}$ ion when

the growth was assayed in batch culture at ambient temperature. This is not entirely unexpected, given the results of the ion competition experiments suggesting that neither $K^+$ nor $Na^+$ could be exported via Yp-NhaP en masse under physiological conditions. The question about exact role of Yp-NhaP in the $Ca^{2+}$ homeostasis needs further investigation.

## 5. FUTURE STUDIES

The present study lays out the groundwork for the future detailed investigation of biochemistry and physiological role of Yp-NhaP. Four possible major lines of study are briefly outlined below.

**(i)** The physiological role of Yp-NhaP *in vivo* remains obscure. The phenotype analysis of the chromosomal deletion mutant presented here did not reveal any influence of the deletion on the growth properties of *Y. pestis*. It must be stressed, however, that we have analyzed only resistance of *Y. pestis* growing in batch culture at ambient temperature to the four cations that are substrates of Yp-NhaP. While the absence of difference in resistance toward alkali cations could be expected (as discussed in above sections), it is possible that at 37ºC the NhaP mutant will display lowered sensitivity to $Ca^{2+}$. It is also possible that the elimination of functional Yp-NhaP could only be revealed in animal model of *Y. pestis* infection, given the tightly closed life cycle of this pathogen.

Also, studies on the regulation of expression of Yp-NhaP could give important information about its physiological role. One may suggest the engineering of a fusion of *Yp-nhaP* with a suitable reporter gene. Such a fusion could be placed into a low-copy number expression plasmid behind the native *nhaP* promoter to monitor the expression of Yp-NhaP in the deletion mutant under different growth conditions.

**(ii)** Only the basic biochemical characterization of Yp-NhaP is presented in this work. In order to complete it, the detailed analysis of mutual influence of different cations on apparent $K_m$ of cation-proton antiport should be performed, starting with a pair "$K^+$-$Na^+$". This will allow to determine whether alkali cations are directly competing for the same set of coordinating ligands. Another immediate task is to check how the addition of $Li^+$ affects the antiport of proton with other substrate cations (and vice versa).

**(iii)** Mutational analysis by means of site-directed mutagenesis could be used to elucidate specific sets of ligands involved in coordination of each of substrate cations. Partial alignment shown in Fig. 1.3 could provide a guidance in the search for mutagenesis targets, but one of the first priorities here should be direct examination of the hypothesis about arginine in position 83 as a structural predictor of the ability of this type of antiporter to mediate $Ca^{2+}/H^+$ antiport. Substitution of this residue by non-polar alanine or other such amino acid is expected to affect (perhaps, even eliminate completely) the ability of Yp-NhaP to bind $Ca^{2+}$ ions.

Also, a series of deletions of C-terminal cytoplasmic tail of Yp-NhaP could be engineered to investigate the role of this cytoplasmic domain of the antiporter in its activity.

**(iv)** Last but not least: All efforts should be made to overexpress and purify Yp-NhaP in its functional form for the structural analysis (including the

attempts of crystallization for the X-ray diffraction analysis) and for its incorporation into proteoliposomes for refined kinetic analysis (for example, direct measurements of $Na^+$ and $Ca^{2+}$ fluxes through Yp-NhaP using corresponding radioactive isotopes of substrate cations). Probably, the most straightforward way of doing it would be the addition of 6×His tag to the C-terminal tail of Yp-NhaP and use the powerful and tightly regulated $P_{BAD}$ promoter of pBAD24 for attenuated overexpression of the tagged antiporter. Overexpressed Yp-NhaP could be then affinity-purified on $Ni^{2+}$-NTA agarose and used for structural and functional studies.

## 6. REFERENCES


Achtman, M., Zurth, K., Morelli, G., Torrea, G., Guiyoule, A. & Carniel, E. (1999). *Yersinia pestis*, the cause of plague, is a recently emerged clone of *Yersinia pseudotuberculosis*. Proc. Natl. Acad. Sci. USA 96:14043–14048.

Bearden, S.W., Fetherston, J.D., and Perry, R.D. (1997) Genetic organization of the yersiniabactin biosynthetic region and construction of avirulent mutants in *Yersinia pestis*. Infect. Immun. 65:1659-1668.

Bogachev, A.V. and Verkhovsky, M.I. (2005) $Na^+$-translocating NADH:quinone oxidoreductase: progress achieved and prospects of investigations. Biochemistry (Moscow) 70(2):143-149.

Brubaker, R. R. (1991). Factors promoting acute and chronic diseases caused by yersiniae. Clin. Microbiol. Rev. 4:309–324.

Brubaker, R.R. (2005) Influence of $Na^+$, dicarboxylic amino acids, and pH in modulating the low-calcium response of *Yersinia pestis*. Infect. Immun. 73:4743-4752.

Brubaker, R.R. (2007) Intermediary metabolism, $Na^+$, the low-calcium response, and acute disease. Adv. Exp. Med. Biol. 603:116-129.

Brubaker, R.R. (2007a) How the structural gene products of *Yersinia pestis* relate to virulence. Future Microbiol. 2(4):377-385.

Cai, X. and Lytton, J. (2004) The cation/$Ca^{2+}$ exchanger superfamily: phylogenetic analysis and structural implications. Mol. Biol. Evol. 21:1692-1703.

Chain, P.S., Carniel, E., Larimer, F. W., Lamerdin, J., Stoutland, P.O., Regala, W.M., Georgescu, A. M., Vergez, L.M., Land, M.L. and other authors (2004) Insights into the evolution of *Yersinia pestis* through whole-genome comparison with *Yersinia pseudotuberculosis*. Proc. Natl. Acad. Sci. USA 101:13826–13831.

Cheng, L.W., Kay, O. and Schneewind, O. (2001) Regulated secretion of YopN by the type III machinery of *Yersinia enterocolitica*. J. Bacteriol. 183:5293–5301.

Cornelis, G.R. and Wolf-Watz, H. (1997) The *Yersinia* Yop virulon: a bacterial system for subverting eukaryotic cells. Mol. Microbiol. 23:861–867.

Datsenko, K.A. and Wanner, B,L. (2000) One-step inactivation of chromosomal genes in *Escherichia coli* K-12 using PCR products. Proc. Natl. Acad. Sci. USA 97:6640-6645.

Day, J.B., Ferracci, F., & Plano, G.V. (2003) Translocation of YopE and YopN into eukaryotic cells by *Yersinia pestis yopN, tyeA, sycN, yscB* and *lcrG* deletion mutants measured using a phosphorylatable peptide tag and phosphospecific antibodies. Mol. Microbiol. 47:807-823.

Desrosiers, M.G., Gately, L.G., Gambel, A.M., & Melnik, D.R. (1996) Purification and characterization of the $Ca^{2+}$-ATPase of *Flavobacterium odoratum*. J. Biol. Chem. 271:3945-3951.

Dzioba-Winogrodzki, J., Winogrodzki, O., Krulwich, T.A., Boin, M.A., Häse, C.C., and Dibrov, P. (2009) Characterization of the *Vibrio cholerae* multifunctional *mrp*-encoded cation/proton antiporter conferring resistance to bile salts in a heterologous host. J. Mol. Microbiol. Biotechnol. 16:176-186.

Fowler, J.M. and Brubaker, R.R. (1994) Physiological basis of the low calcium response in *Yersinia pestis*. Infect Immun 62:5234–5241.

Fowler, J.M, Wulff, C.R., Straley, S.C., and Brubaker, R.R. (2009) Growth of calcium-blind mutants of *Yersinia pestis* at 37°C in permissive $Ca^{2+}$-deficient environments. Microbiology 155:2509-2521.

Francis, M.S., Lloyd, S.A. and Wolf-Watz, H. (2001) The type III secretion chaperone LcrH co-operates with YopD to establish a negative, regulatory loop for control of Yop synthesis in *Yersinia pseudotuberculosis*. Mol. Microbiol. 42:1075–1093.

Galimand, M., A. Guiyoule, G. Gerbaud, B. Rasoamanana, S. Chanteau, E. Carniel, and P. Courvalin (1997) Multidrug resistance in *Yersinia pestis* mediated by a transferable plasmid. N. Engl. J. Med. 337:677–680.

Gambel, A.M., Desrosiers, M.G. and Melnik, D.R. (1992) Characterization of a P-type $Ca^{2+}$ ATPase from *Flavobacterium odoratum*. J. Biol. Chem. 267:15923-15931.

Glusker, P. J., Katz, K. A., and Bock, C. W. (1999) Metal ions in biological systems. The Rigaku Journal. 16:8-17.

Gómez-Puyou, A. and Gómez-Lojero, C. (1977) The use of ionophores and channel formers in the study of the function of biological membranes. Curr. Top. Bioenerg. 6:221-257.

Guffanti, A.A., Cheng, J. and Krulwich, T.A. (1998) Electrogenic antiport activities of the Gram-positive Tet proteins include a $Na^+(K^+)/K^+$ mode that mediates net $K^+$ uptake. J. Biol. Chem. 273: 26447-26454.

Hamada, A., Hibino, T., Nakamura, T., and Takabe, T. (2001) $Na^+/H^+$ antiporter from *Synechocystis* species PCC 6803, homologous to SOS1, contains an aspartic residue and long C-Terminal tail important for the carrier activity. Plant Physiology. 125:437–446.

Hayashi, M., Nakayama, Y., and Unemoto, T. (2001) Recent progress in the $Na^+$-translocating NADH-quinone reductase from the marine *Vibrio alginolyticus*. Biochim. Biophys. Acta 1505(1):37-44.

Häse, C. and Mekalanos, J. (1999) Effects of changes in membrane sodium flux on virulence gene expression in *Vibrio cholerae.* Proc. Natl. Acad. Sci. USA 96:3183-3187.

Heeseman, J., Sing, A., Trülzsch, K. (2006) *Yersinia*'s stratagem: targeting innate and adaptive immune defence. Curr. Opin. Microbiol. 9:1-7.

Hellmer, J., Patzold, R., and Zeilinger, C. (2002) Identification of a pH regulated $Na^+/H^+$ antiporter of *Methanococcus jannaschii*. FEBS Lett. 527:245-249.

Hellmer, J., Teubner, A., and Zeilinger, C. (2003) Conserved arginine and aspartate residues are critical for function of MjNhaP1, a $Na^+/H^+$ antiporter of *M. jannaschii*. FEBS Lett. 524:32-36.

Hu, P., Elliott, J., McCready, P., Skowronski, E., Garnes, J., Kobayashi, A., Brubaker, R.R. & Garcia, E. (1998) Structural organization of virulence-associated plasmids of *Yersinia pestis*. J. Bacteriol. 180:5192–5202.

Hunte, C., Screpanti, E., Venturi, M., Rimon, A., Padan, E. and Michel, H. (2005) Structure of a $Na^+/H^+$ antiporter and insights into mechanism of action and regulation by pH. Nature. 435:1197-1202.

Ivey, D., Guffanti, A., Zemsky, J., Pinner, E., Karpel, R., Padan, E., Schuldiner, S., and Krulwich, T. (1993) Cloning and characterization of a putative $Ca^{2+}/H^+$ antiporter gene from *Escherichia coli* upon functional complementation of $Na^+/H^+$ antiporter-deficient strains by the over expressed gene. J. Biol. Chem. 268:11296–11303.

Kado, C.I. and Liu, S.T. (1981) Rapid procedure for detection and isolation of large and small plasmids. J. Bacteriol. 145:1365-1373.

Kukkonen, M., Suomalainen, M., Kyllonen, P., Lahteenmaki, K., Lang, H., Virkola, R., Helander, I., Holst, O. and Korhonen, T. (2004) Lack of O-antigen is essential for plasminogen activation by *Yersinia pestis* and *Salmonella enterica*. Mol. Microbiol. 51:215–225.

Michiels, T., Wattiau, P., Brasseur, R., Ruysschaert, J.-M., and Cornelis, G. (1990) Secretion of Yop proteins by yersiniae. Infect. Immunol. 58:2840–2849.

Mulkidjanian, A.Y., Dibrov, P. and Galperin, M.Y. (2008) The past and present of sodium energetics: May the sodium-motive force be with you. Biochim. Biophys. Acta. 1777:985-992.

Murata, T., Yamato, I., Kakinuma, Y., Shirouzu, M., Walker, J.E., Yokoyama, S., Iwata, S. (2008) Ion binding and selectivity of the rotor ring of the $Na^+$-transporting V-ATPase. Proc. Natl. Acad. Sci. USA 105(25):8607-8612.

Norris, V., Grant, S., Freestone, P., Canvin, J., *et al*. (1997) Calcium signalling in Bacteria. J. Bacteriol. 178:3677-3682.

Ohyama, T., Igarashi, K. and Kobayashi, H. (1994) Physiological role of the *chaA* gene in sodium and calcium circulation at a high pH in *Escherichia coli*. J. Bacteriol. 176:4311–4315.

Padan, E., Venturi, M., Gerchman, Y., Dover, N. (2001) $Na^+/H^+$ antiporters. Biochim. Biophys. Acta 1505:144-157.

Padan, E., Tzubery, T., Herz, K., Kozachkov, L., Rimon, A., and Galili, L. (2004) NhaA of *Escherichia coli*, as a model of a pH-regulated $Na^+/H^+$ antiporter. Biochim. Biophys. Acta. 1658:2-13.

Padan, E., Bibi, E., Ito, M., and Krulwich, T.A. (2005) Alkaline pH homeostasis in bacteria: new insights. Biochim. Biophys. Acta 1717:67-88.

Padan, E. (2008) The enlightening encounter between structure and function in the NhaA $Na^+$–$H^+$ antiporter, Trends in Biochem. Sci. 33:435-443

Pardo, J. M., Cubero B., Leidi E. O., and Quintero, F. J. (2006) Alkali cation exchangers: roles in cellular homeostasis and stress tolerance. J. Exp. Botany. 57(5):1181-1199.

Perry, R.D. and Brubaker, R.R. (1987) Transport of $Ca^{2+}$ by *Yersinia pestis*. J. Bacteriol. 169:4861–4864.

Perry, R.D and Fetherston, J. (1997) *Yersinia pestis* – etiologic agent of plague. Clin. Microbiol. Rev. 10:35–66.

Pettersson, J., Nordfelth, R., Dubinina, E., Bergman, T., Gustafsson, M., Magnusson, K.-E., and Wolf-Watz, H. (1996) Modulation of virulence factor expression by pathogen target cell contact. Science 273:1231–1233.

Pinner, E., Padan, E. and Schuldiner, S. (1992) Cloning, sequencing, and expression of the *nhaB* gene, encoding a $Na^+/H^+$ antiporter in *Escherichia coli.* J. Biol. Chem. 267:11064-11068.

Pinner, E., Kotler, Y., Padan, E. and Schuldiner, S. (1993) Physiological role of NhaB, a specific $Na^+/H^+$ antiporter in *Escherichia coli.* J. Biol. Chem. 268:1729-1734.

Pinner, E., Padan, E. and Schuldiner, S. (1994) Kinetic properties of NhaB, a $Na^+/H^+$ antiporter from *Escherichia coli.* J. Biol. Chem. 269:26274-26279.

Pinner, E., Padan, E. and Schuldiner, S. (1995) Amiloride and harmaline are potent inhibitors of NhaB, a $Na^+/H^+$ antiporter from *Escherichia coli*. FEBS Lett. 365:18-22.

Pujol, C. & Bliska, J.B. (2003) The ability to replicate in macrophages is conserved between *Yersinia pestis* and *Yersinia pseudotuberculosis*. Infect. Immun. 71:5892-5899.

Radchenko, M.V., Waditee, R., Oshimi, S., Fukuhara, M., Takabe, T., and Nakamura, T. (2006) Cloning, functional expression and primary characterization of *Vibrio parahaemolyticus* $K^+/H^+$ antiporter genes in *Escherichia coli* Mol. Microbiol. 59:651-663.

Resch, C.R., Winogrodzki, J.L., Patterson, C.T., Lind, E.J., Quinn, M.J., Dibrov, P., and Häse, C.C. (2010) The putative $Na^+/H^+$ antiporter of *Vibrio cholerae*, Vc-NhaP2, mediates the specific $K^+/H^+$ exchange in vivo. Biochemistry. 49:2520-2528.

Resch, C.T., Winogrodzki, J.L., Häse, C.C., Dibrov, P. (2011) Insights into the biochemistry of the ubiquitous NhaP family of cation/$H^+$ antiporters. Biochem. and Cell Biol., 89:130-137.

Ruknudin, A. and Schulze, D. (2002) Proteomics approach to $Na^+/Ca^{2+}$ exchangers in prokaryotes. Ann. N.Y. Acad. Sci. 976:103-108.

Saaf, A., Baars, L., von Heijne, G. (2001) The internal repeats in the $Na^+/Ca^{2+}$ exchanger-related *Escherichia coli* protein YrbG have opposite membrane topologies. J. Biol. Chem. 276:18905–18907.

Saier Jr., M. H., Eng, B. H., Fard, S., Garg, J., Haggerty, D. A., Hutchinson, W. J., Jack, D. L., Lai, E. C., Liu, H. J., Nusinew, D. P., Omar, A. M., Pao, S. S.,

Paulsen, I. T., Quan, J. A., Sliwinski, M., Tseng, T., Wachi, S., and Young, G. B. (1999) Phylogenetic characterization of novel transport protein families revealed by genome analyses. Biochim. Biophys. Acta. 1422:1-56.

Sakuma, T., Yamada, N., Saito, H., Kakegawa, T. and Kobayashi, H. (1998) pH dependence of the function of sodium ion extrusion systems in *Escherichia coli*. Biochim. Biophys. Acta 1363:231–237.

Shi, H., Ishitani, M., Kim, C., and Zhu, J. (2000) The *Arabidopsis thaliana* salt tolerance gene *SOS1* encodes a putative $Na^+/H^+$ antiporter. PNAS 97(12):6896-6901.

Shijuku, T., Yamashino, T., Ohashi, H., Saito, H., Kakegawa, T., Ohta, M. and Kobayashi, H. (2002) Expression of chaA, a sodium ion extrusion system of *Escherichia coli*, is regulated by osmolarity and pH. Biochim. Biophys. Acta 1556:142–148.

Soupart, P. (1962) Free amino acids in blood and urine in the human. In: Holden J.T. (ed.) Amino acid pools. Elsevier Publishing Co., Amsterdam, p.220-262.

Tokuda, H. and Unemoto, T. (1982) Characterization of the respiration-dependent $Na^+$ pump in the marine bacterium *Vibrio alginolyticus.* J. Biol. Chem. 257:10007-10014.

Une, T. and Brubaker, R.R. (1984) *In vivo* comparison of avirulent $Vwa^-$ and $Pgm^-$ or $Pst^r$ phenotypes of yersiniae. Infect. Immun. 43:895-900.

Unemoto, T. and Hayashi, M. (1993) $Na^+$-translocating NADH-quinone reductase of marine and halophilic bacteria. J. Bioenerg. Biomembr. 25:385-391.

Utsugi, J., Inaba, K., Kuroda, T., Tsuda, M., and Tsuchiya, T. (1998) Cloning and sequencing of a novel $Na^+/H^+$ antiporter gene from *Pseudomonas aeruginosa*. Biochim. Biophys. Acta. 1398:330-334.

Vinothkumar, K.R., Smits, S.H., and Kühlbrandt, W. (2005) pH-induced structural change in a sodium/proton antiporter from *Methanococcus jannaschii*. EMBO J. 24(15):2720-2729.

Waditee, R., Hibino, T., Tanaka, Y., Nakamura, T., Incharoensakdi, A., and Takabe, T. (2001) Halotolerant cyanobacterium *Aphanothece halophytica* contains an $Na^+/H^+$ antiporter, homologous to eukaryotic ones, with novel ion specificity affected by C-terminal tail. J. Biol. Chem. 276:36931-36938.

Waditee, R., Hossain, G. S., Tanaka, Y., Nakamura, T., Shikata, M., Takano, J. & Takabe, T. (2004) Isolation and functional characterization of $Ca^{2+}/H^+$ antiporters from cyanobacteria. J. Biol. Chem. 279:4330–4338.

Wei, L., Liu, J., Ma, Y., and Krulwich, T. (2007) Three putative cation/proton antiporters from the soda lake alkaliphile *Alkalimonas amylolytica* N10 complement an alkali-sensitive *Escherichia coli* mutant. Microbiology 153:2168-2179.

Wilharm, G., Lehmann, V., Krauss, K., Lehnert, B., Richter, S., Ruckdeschel, K., Heesemann, J. and Trulzsch, K. (2004) *Yersinia enterocolitica* type III secretion depends on the proton motive force but not on the flagellar motor components MotA and MotB. Infect. Immun., 72:4004-4009.